Copy 44
RM SL55D06

NACA

RESEARCH MEMORANDUM

for the

Bureau of Aeronautics, Department of the Navy

TANK INVESTIGATION OF THE HYDRODYNAMIC CHARACTERISTICS OF A 1/13.33-SCALE JET-POWERED DYNAMIC MODEL OF THE MARTIN XP6M-1 FLYING BOAT

TED No. NACA DE 385

By Arthur W. Carter and Ulysse J. Blanchard

Langley Aeronautical Laboratory
Langley Field, Va.

NATIONAL ADVISORY COMMITTEE FOR AERONAUTICS

WASHINGTON

APR 1 1955

NATIONAL ADVISORY COMMITTEE FOR AERONAUTICS

RESEARCH MEMORANDUM

for the

Bureau of Aeronautics, Department of the Navy

TANK INVESTIGATION OF THE HYDRODYNAMIC CHARACTERISTICS OF A 1/13.33-SCALE JET-POWERED DYNAMIC MODEL OF THE MARTIN XP6M-1 FLYING BOAT

TED No. NACA DE 385

By Arthur W. Carter and Ulysse J. Blanchard

SUMMARY

A tank investigation was made of the hydrodynamic characteristics of a 1/13.33-scale jet-powered dynamic model of the 160,000-pound Martin XP6M-1 flying boat. Longitudinal stability during take-off and landing, resistance of the complete model, spray characteristics, flap loads, and effect of sinking speed in smooth and rough water are presented, as well as behavior during taxiing, take-off, and landing in rough water. The effect on spray of two bows and several bow-spray-strip modifications and the effect on resistance of afterbody chine strips also are presented.

INTRODUCTION

A brief investigation of the hydrodynamic characteristics of a preliminary design of the Martin XP6M-1 flying boat was described in reference 1. The results of a transonic wind-tunnel test of this configuration are presented in reference 2. The hydrodynamic investigation indicated a need for revision of the hull lines of the model, particularly in the region of the step. The present investigation, requested by the Bureau of Aeronautics, Department of the Navy, was conducted in order to evaluate the hydrodynamic characteristics of a revised, powered dynamic model which was representative of the final design of the XP6M-1. Tank tests were made of the revised model and of several bow modifications to improve bow spray characteristics in rough water.

The hydrodynamic qualities investigated include longitudinal stability during take-off and landing, resistance of the complete model, spray characteristics, flap hinge moments, and effects of sinking speed in smooth and rough water, as well as behavior during taxiing, take-off, and landing in rough water. The effect of afterbody chine strips on rough-water resistance also was determined.

SYMBOLS

g	acceleration due to gravity, 32.2 ft/sec^2
H.S.	hull station, in.
n_v	vertical acceleration at center of gravity, g units
R	total resistance, lb
V	carriage speed, knots
V_h	horizontal velocity, knots
V_v	vertical velocity (sinking speed), ft/min
W.L.	water line, in.
α	angular acceleration, radians/sec^2
γ	flight-path angle, deg
δ_f	flap deflection, deg
δ_t	stabilizer deflection, deg
Δ_o	gross load, lb
τ	trim (angle between forebody keel at step and horizontal), deg
τ_L	landing trim, deg

DESCRIPTION OF MODEL

The 1/13.33-scale jet-powered dynamic model (Langley tank model 316) is shown in figures 1 and 2. The general arrangement of the seaplane is shown in figure 3. The hull was generally similar to that used in the investigation described in reference 1. The principal changes were an increase in the radius of the curved forebody bottom near the step, installation of the spray strip on the bow radome, addition of spray strips on the tip floats, removal of the step fairing, and close attention to pertinent detail in reproducing the hull lines, particularly in the region of the step. The hull bottom, which was supplied by the Glenn L. Martin Company, was constructed of mahogany and mated to the upper section of the original Fiberglas and plastic model (ref. 1). A Fiberglas and plastic bottom molded from the mahogany bottom was used during parts of the tank investigation.

The wing was the same as that used during the tests described in reference 1, but the tip floats (figs. 1 and 2) were modified to provide more hydrodynamic lift. The lift was increased by adding spray strips to the after portion of the float, not only to increase the beam but also to insure that the water broke cleanly from the chines. The leading edges of the nacelles were cut back to correspond to the latest available information, and afterburners were added. The slats and flap installation were the same as those described in reference 1.

Jet power was simulated by compressed-air nozzles mounted in the nacelle ducts as described in reference 1. The jets provided approximately 45 percent of the scale thrust. Approximately scale air inflow was obtained.

The pitching moment of inertia of the ballasted model was 5.3 slug-feet^2. The ratio of elevator deflection to stabilizer deflection for the all-movable tail was approximately 2.5 to 1.

The following configurations were tested:

<u>Model 316 (figs. 1 and 2)</u> - This model was the basic configuration as received from the Glenn L. Martin Company.

<u>Models 316-1 to 316-9</u> - Bow-spray-strip modifications were formed by adding plastic spray strips to the model. (With the exception of the wide strips of model 316-9, all spray strips were supplied by the Glenn L. Martin Company.)

Model	Figure	Location of strip, in.				Width of strip, in.	Angle to hull, deg
		Forward end		Aft end			
		Station	Water line	Station	Water line		
316-1	4(a)	51	96	80	57	5	60
316-2	4(b)	90	96	119	53	5	45
316-3	4(c)	105	100	135	60	5	60
316-4	4(d)	47	75	142	65	6	90
316-5	4(e)	90	96	150	51	6.5	90
316-6	[a]4(f)	90	96	150	51	7	45
316-7	[a]4(g)	65	96	138	52	5	45
316-8	[b]4(h)	65	96	138	52	5	45
316-9	4(i)	30	93	213	54	10	90

[a]In addition, a vertical chine strip extended downward 6.5 inches from station 96 to station 290.

[b]The vertical chine strips of model 316-7 were set at 45° to the horizontal.

Model 316-10 (fig. 4(j)) - The chines of the basic model were extended forward to hull station 30.

Model 316-11 (fig. 4(k)) - This model was the same as model 316-10 with a vertical chine strip extending downward 1.5 inches from station 30 to station 350.

Model 316-12 (fig. 5(a)) - A 3.33-inch-wide horizontal spray strip was added to the afterbody of the basic hull. These strips were located approximately at the point of maximum beam and extended from hull station 685 to station 1,026.

Model 316-13 (fig. 5(b)) - The afterbody spray strips of model 316-12 were extended aft to hull station 1,426.

Model 316A (fig. 6) - The bow and chines were extended 39.2 inches (full size) forward of basic hull station 0, and the bow radome was eliminated. Hull lines aft of station 212 were the same as those of model 316. This modification, designated the "hydrodynamic bow," was of built-up construction and was designed and supplied by the Glenn L. Martin Company. The pitching moment of inertia of the ballasted model with the hydrodynamic bow was 4.5 slug-feet^2.

APPARATUS

The investigation was made in Langley tank no. 1, which is described in reference 3. The apparatus generally used for testing dynamic models is described in references 4, 5, and 6. The setup of a model on the towing apparatus is shown in figure 7.

A schematic drawing of the setup used to determine the resistance in rough water is shown in figure 8. A force pickup (strain gage) was attached to the front of the roller cage of the fore-and-aft gear. Long rubber strands attached to the force pickup had a spring constant of about 1.5 pounds per foot.

The setup used during free-body landings is shown in figure 9. The model was towed from two brackets located on the wing. A tail support prevented the model from changing trim prior to launching. The wing brackets were slotted so that, with a sudden deceleration of the towing carriage, the inertia of the model caused the model to fly free of the gear.

PROCEDURE

All data were obtained at a gross load corresponding to 160,000 pounds, with a flap deflection of 40°, and with the center of gravity located at 28.5 percent mean aerodynamic chord unless noted otherwise.

Trim limits of stability.- The trim limits of stability were determined without power at constant speeds by use of the methods described in reference 4. The trims at which porpoising started were observed and recorded.

Accelerated take-offs.- The longitudinal stability during take-off in smooth and rough water for various tail settings was determined by making accelerated runs up to take-off speed with power and a constant rate of acceleration of 3.5 feet per second per second. Because the jets provided only 45 percent of scale thrust, a weight moment was added to provide the additional pitching moment associated with full-scale thrust. The trim, rise, accelerations, and speed of the model were recorded.

Landings with fore-and-aft gear.- The landing stability in smooth water and the landing behavior in waves were investigated with the model free to move fore and aft. The model was trimmed in the air to the desired landing trim at a speed slightly above flying speed and the towing carriage was decelerated at a uniform rate; this technique allowed the model to glide onto the water and simulate an actual landing. The landings were made without power. During landings in smooth water, the tail surfaces were set so that the model was in trim at the instant of contact. The landings in rough water were made at a trim of 12° with the tail surfaces set for a trim of 8°, so that a bow-down aerodynamic moment was applied immediately upon contact with the water. In order to maintain longitudinal freedom, the rates of deceleration were approximately 6.5 and 8 feet per second per second in smooth and rough water, respectively. Landings were made in waves 4, 6, and 8 feet in height (full size). The initial landing approach was made with the sternpost 8 inches above the static water level. After initial contact, the model was allowed vertical movement to a height of 28 inches above the static water level.

In order to determine the effect of high sinking speed on the landing behavior, landings were made with the initial sinking speed increased to approximately 1,500 feet per minute (full size). With the forward speed slightly below flying speed, the model was locked against the rise stop. Air pressure was applied to the rise-stop cylinder to give the model an initial downward force. As the carriage began to make the decelerated run, a bomb release attached to the cable supporting the model was tripped. After the initial force was applied by the compressed air, the model was free of the rise stop and no additional external force was applied as the model made the landing.

Trim, rise, fore-and-aft position, accelerations, and speed were recorded.

Free-body landings.- Free-body landings were made in smooth water and in waves. The model was towed in the air at the desired landing trim and at a speed slightly above flying speed. By suddenly applying brakes to the towing carriage, the model was launched ahead of the carriage as a free body. The behavior of the model was photographed and visual observations were made.

Spray characteristics.- The spray characteristics in smooth water and waves were determined from visual observations and from motion pictures of taxiing, take-offs, and landings.

Flap hinge moment.- The flap hinge moments were determined during take-off in smooth water and during taxiing and landing in waves. The output from the strain gage and the speed were recorded.

Resistance.- The free-to-trim resistance of the complete model was determined at constant speeds. In smooth water, a sufficient number of tail deflections were investigated to determine the minimum resistance for stable trims at each speed. In rough water, the force pickup attached to the roller cage was used to measure the total resistance. At each constant speed, the tension in the strands of rubber was adjusted by means of a winch on the towing carriage until the model was free of the stops on the fore-and-aft gear. The total resistance as indicated by the force pickup was then recorded.

RESULTS AND DISCUSSION

All test results have been converted to values corresponding to the full-size flying boat.

Trim limits of stability.- The trim limits of stability for the basic model (tank model 316) are presented in figure 10. An intermediate region of mild instability was noted just above the lower limit. Similar porpoising was noted during the investigation described in reference 1. Sufficient data were not obtained to define this region. When the upper limit, increasing trim, was encountered, the afterbody appeared to stick, and a large bow-down aerodynamic moment was required to recover from upper-limit porpoising. When a sufficient moment was applied, the model would recover but, because of the sudden change in trim, the values for the upper limit, decreasing trim, could not be obtained accurately.

At speeds near take-off, the trim limits were indeterminable for the basic hull. Divergent porpoising was encountered in accelerating to these speeds before a constant speed could be obtained. Recovery from this porpoising could not be made by use of the tail surfaces, and the test runs had to be discontinued.

With afterbody chine strips (model 316-12), stable constant-speed runs were possible at all speeds up to getaway.

Accelerated take-offs.- The variation of trim with speed during take-off in smooth water is shown in figure 11 for the basic model with various stabilizer settings. At low stabilizer settings ($\delta_t = -4.5^{\circ}$ to -6°), the trim remained above the lower limit but intermediate porpoising (small amplitude and nondivergent) between the limits was encountered. At higher stabilizer settings ($\delta_t = -6.5^{\circ}$ to -9.5°), upper-limit porpoising was encountered. In general, the take-off stability appeared to be satisfactory and porpoising amplitudes did not exceed 2.2° for stabilizer settings below -6.5°.

The data obtained during take-offs in 2-, 4-, and 6-foot waves are presented in table I. The variation of trim and rise with speed for a typical take-off in 4-foot waves is shown in figure 12. A comparison of the take-off data with the landing data (tables II, III, and IV) indicates that the maximum vertical and angular accelerations and the motions in trim were approximately the same for take-off as for landing.

Landings with fore-and-aft gear.- Typical time histories of trim, rise, and speed during landings in smooth water are presented in figure 13. The maximum variation of trim and rise and the number of skips (hull left the water) are presented in figure 14 for various landing trims. The trim and rise cycles were small at landing trims below 10°. At landing trims above 10°, the model landed above the upper trim limit and porpoising was encountered. This porpoising increased the magnitude of the trim and rise cycles, but the motions were not violent. In general, the landing stability in smooth water was excellent.

Pertinent data for the impact which resulted in the maximum acceleration during each landing in waves are given in tables II, III, and IV for wave heights of 4, 6, and 8 feet, respectively.

The effect of wave length on the rough-water landing characteristics in 4-, 6-, and 8-foot waves is presented in figures 15(a), 15(b), and 15(c), respectively. The maximum vertical and angular accelerations for each landing and the trim and rise at the greatest cycle are plotted against wave length. In general, the accelerations, trim, and rise did not vary greatly with wave length. At the critical wave length (wave length at which the maximum acceleration occurred), an increase in wave height from 4 feet to 6 feet increased the maximum vertical and angular accelerations approximately 30 percent; an increase in wave height from 4 feet to 8 feet increased the maximum vertical and angular accelerations approximately 50 and 60 percent, respectively.

Effect of high sinking speed on landing behavior.- The effect of high sinking speed on the landing behavior in smooth water is shown in figure 16(a). The trim and rise cycles were greatly increased by an increase in initial sinking speed from 335 to 1,465 feet per minute. The effect of the high sinking speed on the motions in trim and rise persisted during a large part of the landing run.

Pertinent data obtained during landings at the critical wave length are given in table V and are plotted in figure 16(b) for wave heights of 4, 6, and 8 feet. The higher sinking speed caused a considerable increase in both the accelerations and the motions. In order to avoid damage to the model, landings in 8-foot waves with the high sinking speed were discontinued after one landing.

Free-body landings.- Free-body landings were made at gross loads of 123,000 and 160,000 pounds in smooth water and in waves 2, 4, and 6 feet high. The behavior and motions of the model during these landings appeared to be similar to those obtained during landings in the fore-and-aft gear. No evidence of directional instability was noted. After one landing in 6-foot waves, the test was discontinued because the deceleration of the model was greater than that of the towing carriage (14 feet per second per second) from which the model was launched.

Spray characteristics.- In smooth water, the windshield and duct inlets of the basic model were clear of spray at all speeds. Water flowed over the wing tips just inboard of the tip floats up to a speed of 45 knots. Spray struck the afterburners at speeds between 45 and 60 knots. Spray on the 40° flaps was heavy over the speed range from 30 to 65 knots. A typical spray pattern at a speed of approximately 70 knots in smooth water is shown in figure 7.

In rough water, the spray entered the duct inlets of the basic model at all wave heights investigated. In 4-foot waves the windshield was wetted, and in 6- and 8-foot waves the spray covered a large portion of the wing.

In general, the various bow spray strips (models 316-1 to 316-8) eliminated the spray from the inboard duct inlets in waves up to 8 feet high and from the outboard inlets in 2-foot waves. For most of these configurations, spray entered the outboard inlets in 4-, 6-, and 8-foot waves. The diagonal strips on model 316-5 appeared to be the most effective in reducing the spray entering the duct inlets. Vertical chine strips in combination with the diagonal strips (models 316-6 to 316-8) had little effect on the amount of spray entering the inlets.

The wide spray strips of model 316-9 eliminated spray in the inlets in the 2- and 4-foot waves and the spray in the outboard ducts was light in 6- and 8-foot waves. This modification gave an indication of the size of strip required to have an appreciable effect on the spray entering the outboard inlets.

The spray characteristics of the configuration having an extended chine (models 316-10 and 316-11) appeared to be approximately the same as those of the basic model.

With the "hydrodynamic bow" (model 316A), the inboard duct inlets were clear of spray in waves up to 6 feet in height and the outboard inlets were clear of spray in waves up to 2 feet in height. In 8-foot waves, heavy spray entered all inlets.

Flap hinge moments.- The variations of trim, rise, and flap hinge moment with speed in smooth water are shown in figure 17 for flap deflections of 10° and 40°.

The variation of flap hinge moment with speed during power-on taxiing in waves is shown in figure 18(a) for a flap deflection of 10°. The maximum hinge moment was obtained at approximately 55 knots in all wave heights.

The variation of flap hinge moment with speed during landings in 4- and 6-foot waves is shown in figure 18(b). These data are for one landing at each wave height.

Resistance.- The total resistance and trim for the basic model in smooth water are presented in figure 19. The solid lines represent the minimum total resistance and the trim for minimum resistance.

The effect of wave height on the average total resistance was determined for model 316-5 in 2-, 4-, and 6-foot waves. Data are presented in figures 20(a), 20(b), and 20(c) for flap deflections of 0°, 10°, and 40°, respectively. The resistance in smooth water would be substantially the same as that of the basic model (fig. 19) since the bow strips were not wetted except at very low speeds. The resistance in 2-foot waves was slightly greater than that in smooth water but increased rapidly with further increase in wave height. A comparison of the resistance with the three flap deflections indicated that 40° flaps were not advantageous at speeds below 90 knots.

The effect of gross load on the total resistance in 4-foot waves is shown in figure 21. At hump speed, the total resistance at the lightest load (140,000 pounds) was approximately 25 percent less than that of the heavier loads (160,000 pounds and 180,000 pounds). At intermediate planing speeds, the increase in total resistance with gross load was uniform.

The effect of wave length on the total resistance in rough water is shown in figure 22. An increase in wave length reduced the total resistance in both 4- and 6-foot waves.

The effect of afterbody strips on the total resistance in waves is shown in figures 23 and 24 for models 316-12 (short strips) and 316-13 (long strips), respectively. In general, the effects of afterbody strips were small and indefinite.

CONCLUDING REMARKS

Tank tests of a 1/13.33-scale dynamic model of the Martin XP6M-1 flying boat indicate that the longitudinal stability during take-off was satisfactory and the longitudinal stability during landing was excellent. The maximum accelerations and the motions in trim were approximately the same for take-off and landing in waves. High sinking speed greatly increased the accelerations and motions in trim and rise. No evidence of directional instability was noted during free-body landings in smooth and rough water. In smooth water, the windshield and duct inlets of the basic model were clear of spray at all speeds. In waves, spray entered the duct inlets of the basic model at all wave heights. In general, the various bow-strip modifications eliminated the spray from the inboard duct inlets in waves up to 8 feet high and from the outboard inlets in 2-foot waves. The average resistance in 2-foot waves was slightly greater than that in smooth water but increased rapidly with further increase in wave height.

Langley Aeronautical Laboratory,
National Advisory Committee for Aeronautics,
Langley Field, Va., March 18, 1955.

Arthur W. Carter
Aeronautical Research Scientist

Ulysse J. Blanchard
Aeronautical Research Scientist

Approved: John B. Parkinson
Chief of Hydrodynamics Division

mgk

REFERENCES

1. Blanchard, Ulysse J.: A Brief Investigation of the Hydrodynamic Characteristics of a 1/13.33-Scale Powered Dynamic Model of a Preliminary Design of the Martin XP6M-1 Flying Boat - TED No. NACA DE 385. NACA RM SL53K06, Bur. Aero., 1953.

2. Hieser, Gerald, Kudlacik, Louis, and Gray, W. H.: A Transonic Wind-Tunnel Investigation of a Seaplane Configuration Having a 40° Swept-back Wing - TED No. NACA DE 387. NACA RM SL55D07, Bur. Aero., 1955.

3. Truscott, Starr: The Enlarged N.A.C.A. Tank, and Some of Its Work. NACA TM 918, 1939.

4. Olson, Roland E., and Land, Norman S.: Methods Used in the NACA Tank for the Investigation of the Longitudinal-Stability Characteristics of Models of Flying Boats. NACA Rep. 753, 1943. (Supersedes NACA WR L-409.)

5. Carter, Arthur W.: Effect of Hull Length-Beam Ratio on the Hydrodynamic Characteristics of Flying Boats in Waves. NACA TN 1782, 1949.

6. Carter, Arthur W., West, Max D., and Bryce, Paul W., Jr.: An Investigation of the Hydrodynamic Characteristics of a Jet-Powered Dynamic Model of the DR 56 Flying Boat - TED No. NACA DE 328. NACA RM SL51A03, Bur. Aero., 1951.

TABLE I.- DATA OBTAINED DURING TAKE-OFFS

IN WAVES FOR MARTIN XP6M-1 FLYING BOAT

[All values are full size]

[redacted]

Take-off	Wave height, ft	Wave length, ft	Maximum acceleration					
			τ, deg	V_v, ft/min	V_h, knots	γ, deg	n_v, g units	α, $\frac{\text{radians}}{\text{sec}^2}$
1	2	200	3.2	800	113.0	4.00	2.1	2.0
2	2	200	2.8	857	116.0	4.17	2.4	2.3
3	2	200	4.1	942	112.1	4.75	3.1	---
4	2	200	4.7	703	114.0	3.48	2.5	---
5	2	200	2.3	762	105.8	4.07	2.4	---
6	2	200	3.0	857	104.7	4.62	2.9	---
7	4	200	5.2	335	109.3	1.73	2.1	2.9
8	4	200	5.4	771	119.2	3.65	4.2	3.9
9	4	200	4.7	668	121.0	3.12	3.0	3.5
10	4	200	3.3	605	110.8	3.08	3.1	3.9
11	4	200	5.0	705	120.8	3.30	4.5	4.5
12	4	200	6.5	697	97.4	4.05	3.3	4.0
13	4	200	5.6	521	108.0	2.73	2.3	3.2
14	4	200	4.9	605	123.8	2.76	2.6	3.1
15	4	200	6.0	605	122.5	2.79	3.3	3.6
16	4	200	3.7	1,139	114.5	5.62	5.0	---
17	4	200	4.7	892	117.5	4.28	4.5	---
18	6	200	7.5	968	112.5	4.84	5.8	---
19	6	200	4.7	881	117.5	4.23	5.0	---
20	6	200	6.2	412	122.9	1.90	3.4	---

[redacted]

TABLE II.- DATA OBTAINED DURING LANDINGS IN WAVES

4 FEET HIGH FOR MARTIN XP6M-1 FLYING BOAT

[All values are full size]

Landing	Wave length, ft	Maximum acceleration						
		Impact	τ, deg	V_v, ft/min	V_h, knots	γ, deg	n_v, g units	α, $\frac{\text{radians}}{\text{sec}^2}$
1	173	2	4.5	1,255	106.5	6.65	4.6	4.9
2	173	1	5.1	583	121.2	2.72	4.2	4.9
3	173	3	6.4	248	111.2	1.27	3.2	2.9
4	173	2	3.4	1,249	109.1	6.45	5.0	5.8
5	173	4	6.0	1,271	98.9	7.23	4.6	4.7
6	173	2	3.3	1,288	126.2	5.77	4.7	4.0
7	173	6	6.6	1,003	83.1	6.80	3.4	4.0
8	173	3	8.5	960	98.0	5.52	3.6	2.5
8	173	[a]2	2.4	743	112.5	3.73	3.3	4.4
9	173	2	4.9	999	106.7	5.28	4.1	4.0
10	200	3	4.8	999	107.6	5.25	4.3	4.4
11	200	4	7.5	1,183	98.7	6.75	4.3	3.2
12	200	7	6.3	931	94.8	5.53	3.4	3.6
13	200	6	5.1	1,078	80.9	7.50	3.5	5.4
14	200	1	4.6	556	122.7	2.57	3.4	3.6
15	200	1	4.4	609	122.7	2.80	2.9	3.2
16	200	2	2.9	1,420	107.1	7.47	5.6	7.2
17	200	3	7.1	1,205	99.3	6.83	4.6	4.0
18	240	1	5.5	302	135.5	1.27	2.0	.9
19	240	1	4.6	379	135.5	1.58	2.8	2.6
20	240	4	4.6	979	111.7	4.95	2.6	1.8
21	240	3	5.7	541	125.1	2.45	2.3	1.8
22	240	2	4.1	1,065	111.5	5.38	3.4	4.4
23	240	3	3.5	1,212	93.3	7.32	4.3	5.8
24	240	3	4.6	602	111.7	3.05	2.7	3.6
25	240	3	4.5	607	111.9	3.07	2.7	3.6
26	240	1	4.7	716	139.4	2.90	3.4	3.1
27	240	3	4.1	1,288	107.1	6.77	4.6	4.4
28	240	1	4.9	688	124.2	3.13	2.6	2.9
29	240	1	3.5	539	122.3	2.50	2.5	3.6
30	280	2	5.0	1,170	121.6	5.43	2.6	1.5
31	280	2	4.2	646	124.2	2.95	2.8	2.3
32	280	3	5.4	1,047	101.1	5.85	3.2	3.1
33	280	3	5.1	1,319	94.6	7.85	3.5	3.2
34	280	4	3.5	1,301	92.4	7.92	4.0	5.1
35	280	4	5.4	988	90.5	6.15	2.7	3.2
36	280	3	6.5	911	103.4	4.97	2.9	1.6
36	280	[a]2	5.3	616	117.1	2.97	2.5	2.5
37	280	2	5.9	629	121.6	2.92	2.4	2.6
38	280	2	4.2	624	113.0	3.12	2.5	3.1
39	280	3	5.5	800	109.1	4.15	2.1	2.2
40	320	2	3.0	905	109.1	4.68	4.5	5.4
41	320	1	5.3	666	124.9	3.02	2.3	2.3
42	320	1	5.1	605	125.1	2.73	2.8	3.3
43	320	3	5.7	734	108.8	3.82	3.3	3.2
44	320	5	6.1	1,038	76.6	7.63	2.6	2.9
45	320	1	3.2	725	117.7	3.48	2.4	4.1
46	320	1	3.7	664	116.4	3.22	2.4	3.3
47	320	2	3.8	1,499	101.3	8.32	3.3	2.6
47	320	[a]1	3.4	767	117.5	3.68	2.6	3.7

[a]Impact for maximum angular acceleration.

TABLE III.- DATA OBTAINED DURING LANDINGS IN WAVES

6 FEET HIGH FOR MARTIN XP6M-1 FLYING BOAT

[All values are full size]

Landing	Wave length, ft	Maximum acceleration						
		Impact	τ, deg	V_v, ft/min	V_h, knots	γ, deg	n_v, g units	α, $\frac{\text{radians}}{\text{sec}^2}$
1	200	2	6.1	1,354	103.0	7.40	7.1	6.7
2	200	6	4.5	1,424	74.4	10.70	4.4	7.1
3	200	2	4.8	916	106.9	4.83	5.9	5.4
3	200	[a]4	3.5	1,209	80.5	8.43	4.7	7.8
4	200	4	5.9	1,325	92.6	8.05	6.7	9.4
5	200	3	5.0	1,320	91.3	8.13	6.0	8.8
6	200	3	2.2	966	103.9	5.25	5.6	8.4
7	200	2	6.9	1,172	102.8	6.42	5.4	4.4
8	240	6	7.7	927	97.4	5.37	3.9	2.8
9	240	4	10.4	1,177	86.6	7.65	3.9	1.3
9	240	[a]2	3.3	751	122.9	3.45	3.2	3.7
10	240	3	5.9	1,648	100.2	9.23	5.2	3.8
11	240	1	4.4	581	124.6	2.63	4.4	4.5
12	240	1	4.0	675	123.3	3.10	4.3	5.4
13	240	6	5.1	1,332	81.2	9.22	4.4	5.4
14	240	1	3.2	633	123.8	2.90	4.0	5.4
15	240	4	4.5	649	105.4	3.48	3.1	4.2
16	240	1	4.0	662	119.0	3.15	4.3	7.0
17	240	2	4.8	1,365	106.7	7.20	4.6	5.0
18	260	3	6.9	1,141	89.2	7.22	4.5	5.1
19	260	3	4.0	708	108.6	3.68	3.5	4.7
20	260	6	6.1	1,433	86.1	9.33	4.2	4.9
21	260	2	10.9	1,792	100.2	10.02	4.2	.9
21	260	[a]1	4.0	747	117.5	3.60	3.3	4.9
22	260	2	7.2	1,244	103.7	6.77	5.7	5.1
23	260	2	8.3	1,187	103.0	6.50	4.7	3.5
23	260	[a]1	4.3	624	120.8	2.93	3.9	4.7
24	260	2	4.2	524	112.1	2.65	3.4	2.9
25	260	1	5.9	605	124.0	2.33	4.3	4.0
26	280	4	7.4	1,433	90.0	8.93	5.2	3.5
26	280	[a]2	2.7	894	121.6	4.15	4.8	5.3
27	280	4	6.7	714	112.5	3.58	3.5	3.4
28	280	2	4.1	1,470	118.6	6.98	6.0	6.4
29	280	3	4.2	1,144	116.9	5.52	5.1	5.5
30	280	1	3.4	723	125.1	3.27	3.8	5.4
31	280	2	2.5	1,314	111.7	6.63	5.2	6.9
32	280	3	3.2	1,397	108.8	7.23	6.3	7.2
33	280	2	3.4	1,328	108.0	6.93	5.0	4.7
34	280	2	3.5	552	107.3	2.90	6.5	6.4
35	280	2	3.5	1,205	109.1	6.23	5.2	6.2
36	280	2	4.4	1,490	102.4	8.18	5.3	5.5
37	280	2	3.3	1,295	105.2	6.93	5.4	7.1
38	320	2	4.4	1,372	118.2	6.53	5.2	5.9
39	320	5	3.8	1,190	92.4	7.25	4.5	4.7
40	320	4	8.0	1,413	94.8	8.37	5.2	3.5
40	320	[a]3	3.6	833	109.7	4.30	3.6	5.1
41	320	3	2.8	1,420	105.8	7.55	6.0	8.0
42	320	3	2.5	1,718	104.7	9.20	5.4	6.9
43	320	1	5.4	600	121.2	2.80	3.1	2.9
44	320	3	5.3	1,334	90.0	8.33	5.8	5.8
45	320	3	3.2	828	106.0	4.42	6.2	7.5
46	320	2	5.4	1,385	102.6	7.60	5.3	5.5
47	320	4	4.4	1,179	90.0	7.38	4.2	4.1
48	320	2	4.4	1,621	101.3	8.98	5.8	6.2
49	360	2	5.5	1,341	119.0	6.35	5.1	4.7
50	360	2	5.8	1,183	118.6	5.63	4.4	3.6
51	360	3	4.0	1,218	102.1	6.72	3.6	4.4
52	360	3	4.0	1,525	93.5	9.15	5.7	6.9
53	360	1	3.3	793	120.1	3.73	2.9	4.3
54	360	1	3.6	857	121.6	3.98	2.9	4.3
55	360	1	7.5	583	122.3	2.70	3.0	2.1
56	360	4	5.9	911	88.9	5.78	2.9	3.2
57	360	1	3.2	712	122.7	3.28	3.4	4.4

[a]Impact for maximum angular acceleration.

TABLE IV.- DATA OBTAINED DURING LANDINGS IN WAVES

8 FEET HIGH FOR MARTIN XP6M-1 FLYING BOAT

[All values are full size]

Landing	Wave length, ft	Maximum acceleration						
		Impact	τ, deg	V_V, ft/min	V_h, knots	γ, deg	n_V, g units	α, $\frac{radians}{sec^2}$
1	200	3	4.4	1,297	88.5	8.23	6.0	10.9
2	200	1	6.3	631	121.4	2.93	3.0	2.2
3	200	2	5.1	1,516	100.0	8.52	5.5	8.5
4	200	1	4.5	806	119.9	3.80	5.2	5.0
5	200	3	6.6	957	107.6	5.02	4.7	3.2
6	200	5	4.8	1,415	94.6	8.42	6.8	8.7
7	240	3	5.5	1,490	103.7	8.08	7.3	9.9
8	240	4	2.6	1,293	84.0	8.65	5.4	9.0
9	240	4	3.5	1,702	91.5	10.42	8.3	11.4
10	240	3	12.3	1,551	89.4	9.73	4.9	1.8
10	240	[a]1	4.0	692	123.8	3.17	4.7	8.3
11	240	3	6.6	1,021	105.6	5.45	4.5	4.0
12	240	6	3.8	916	89.8	5.77	5.3	7.7
13	240	2	5.2	1,799	106.9	9.43	7.2	9.4
14	240	4	6.7	1,660	90.0	10.33	5.4	7.2
15	280	3	3.9	659	106.9	3.48	3.9	5.7
16	280	3	5.1	1,293	107.3	6.78	6.7	6.2
17	280	2	7.7	1,584	103.2	8.62	7.6	6.7
17	280	[a]3	3.5	1,407	92.0	8.58	6.0	8.5
18	280	2	4.4	1,144	111.0	5.82	6.1	6.5
19	280	4	4.7	1,363	86.3	8.87	5.8	8.3
20	280	1	3.3	813	123.3	3.73	5.5	7.2
21	280	2	4.4	1,146	111.0	5.82	5.2	7.2
22	280	5	5.2	1,385	87.6	8.87	4.6	7.2
23	320	1	2.8	859	123.1	3.93	7.2	6.4
24	320	4	4.4	1,921	80.1	13.33	4.5	5.8
25	320	2	9.0	1,575	100.6	8.78	6.9	4.7
25	320	[a]3	3.6	1,591	81.2	10.95	4.1	7.2
26	320	2	7.2	2,364	98.5	13.33	7.0	6.9
26	320	[a]1	3.1	830	119.9	3.92	5.4	8.7
27	320	1	5.9	668	122.7	3.08	3.5	3.1
27	320	[a]3	3.6	988	108.2	5.15	2.8	4.0
28	320	3	6.5	1,479	101.7	8.17	7.1	7.2
29	320	2	4.0	1,545	96.9	8.95	6.2	8.7
30	360	5	7.9	732	71.0	5.82	3.8	2.2
31	360	1	2.8	885	121.2	4.13	5.0	7.2
32	360	3	7.7	1,652	93.1	9.95	5.7	4.4
32	360	[a]2	3.2	890	110.8	4.53	2.8	5.4
33	360	1	4.8	745	121.4	3.47	4.4	5.1
34	360	2	4.8	738	112.3	3.72	3.3	4.0
35	360	1	3.5	843	121.8	3.92	3.8	5.1
36	360	6	9.7	760	87.0	4.93	2.4	1.8

[a]Impact for maximum angular acceleration.

TABLE V.- DATA OBTAINED DURING LANDINGS WITH HIGH INITIAL SINKING SPEED IN WAVES FOR MARTIN XP6M-1 FLYING BOAT

[All values are full size]

Landing	Wave height, ft	Wave length, ft	Maximum acceleration						
			Impact	τ, deg	V_v, ft/min	V_h, knots	γ, deg	n_v, g units	α, $\frac{radians}{sec^2}$
1	4	200	3	-2.8	1,709	110.4	8.70	6.2	8.7
2	4	200	3	-2.3	1,293	110.8	6.58	5.9	8.0
2	4	200	[a]2	-.6	1,363	129.8	5.92	5.6	9.0
3	4	200	3	-2.3	1,814	113.4	8.98	5.4	8.5
4	4	200	2	-3.0	1,615	123.1	7.38	5.6	6.2
5	4	200	3	-2.8	1,766	106.0	9.35	6.9	8.7
6	4	200	4	2.3	1,534	92.4	9.32	4.8	8.0
7	6	200	3	-1.5	1,363	124.2	6.18	7.6	10.5
8	6	200	2	1.2	1,336	125.5	5.98	5.1	5.3
9	6	200	1	4.8	1,520	130.5	6.57	6.3	5.4
10	6	200	1	4.8	1,586	127.2	7.02	7.9	8.7
11	6	200	1	5.4	1,650	123.8	7.50	6.7	6.2
11	6	200	[a]2	.8	1,656	102.1	9.10	6.0	10.9
12	6	200	3	-2.4	1,963	101.9	10.78	7.5	12.3
13	6	200	1	5.5	1,560	125.5	7.00	7.4	8.3
14	6	200	3	-3.6	1,963	105.4	10.43	6.9	11.3
15	8	240	3	4.1	1,871	102.6	10.13	9.5	14.1

[a]Impact for maximum angular acceleration.

[redacted]

[redacted]

[redacted]

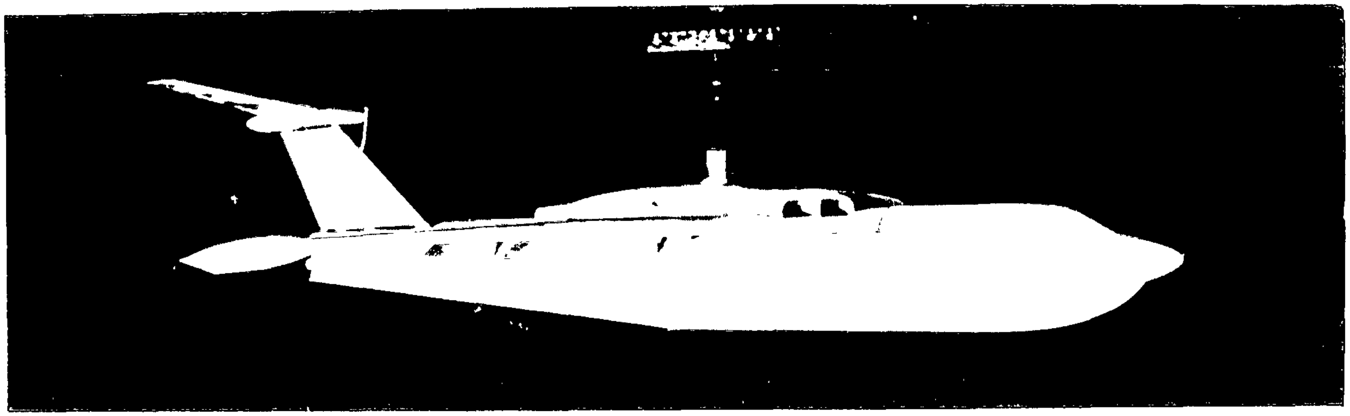

Three-quarter front view

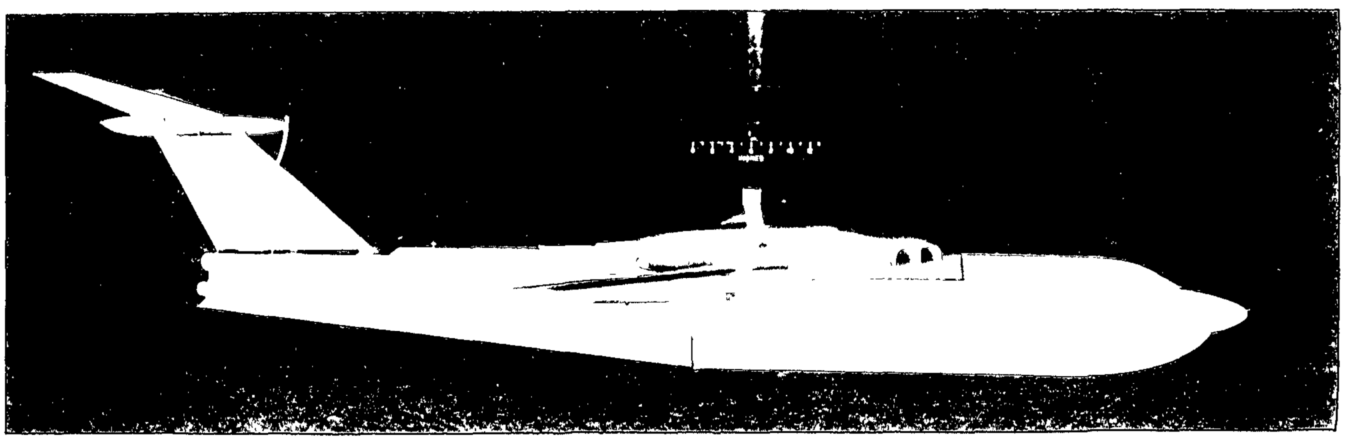

Profile view

Figure 1.- Langley tank model 316.

L-87919

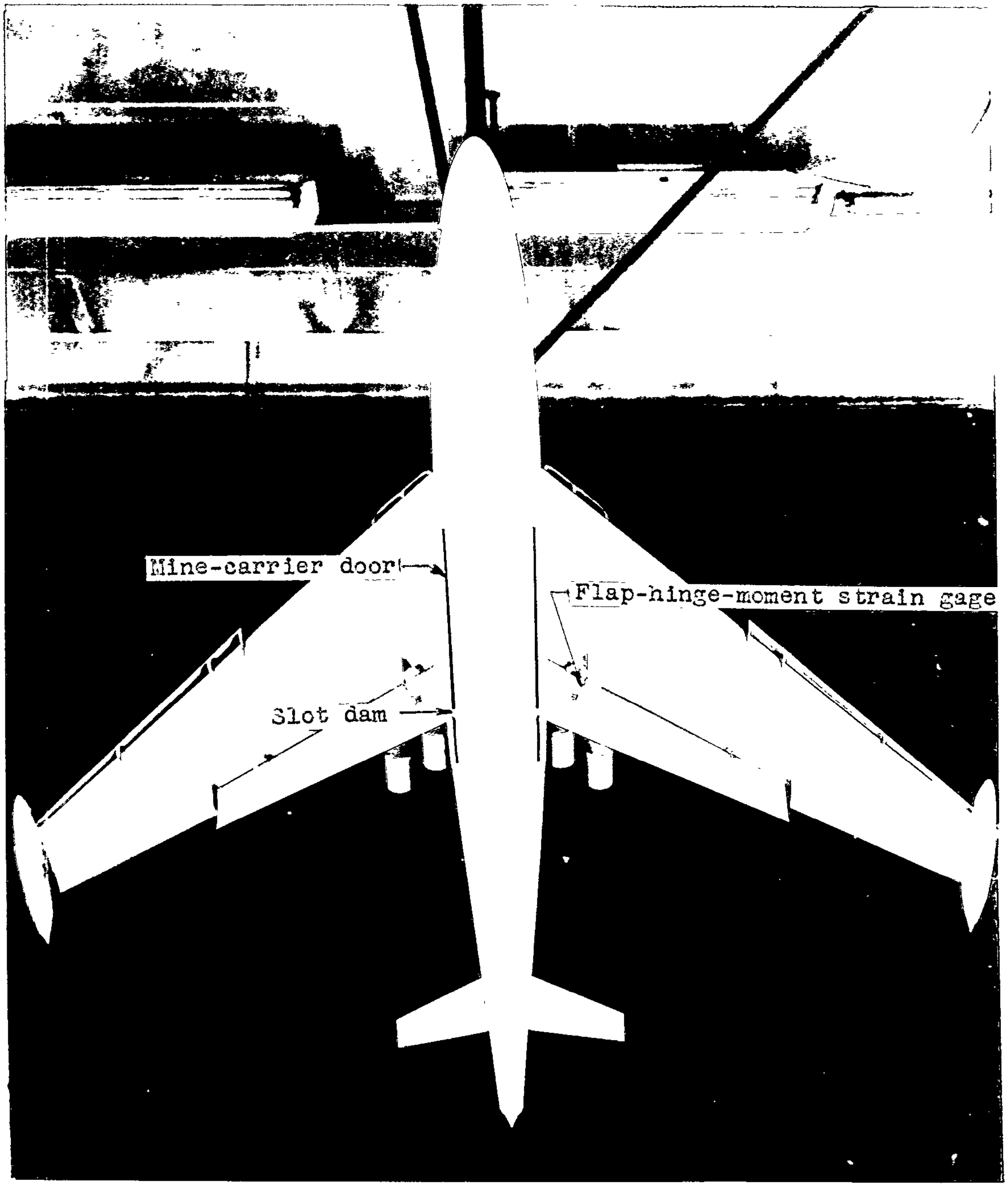

L-82514.1

Figure 2.- Langley tank model 316. Bottom view showing mine-carrier door, slot dam, and flap-hinge-moment strain gage.

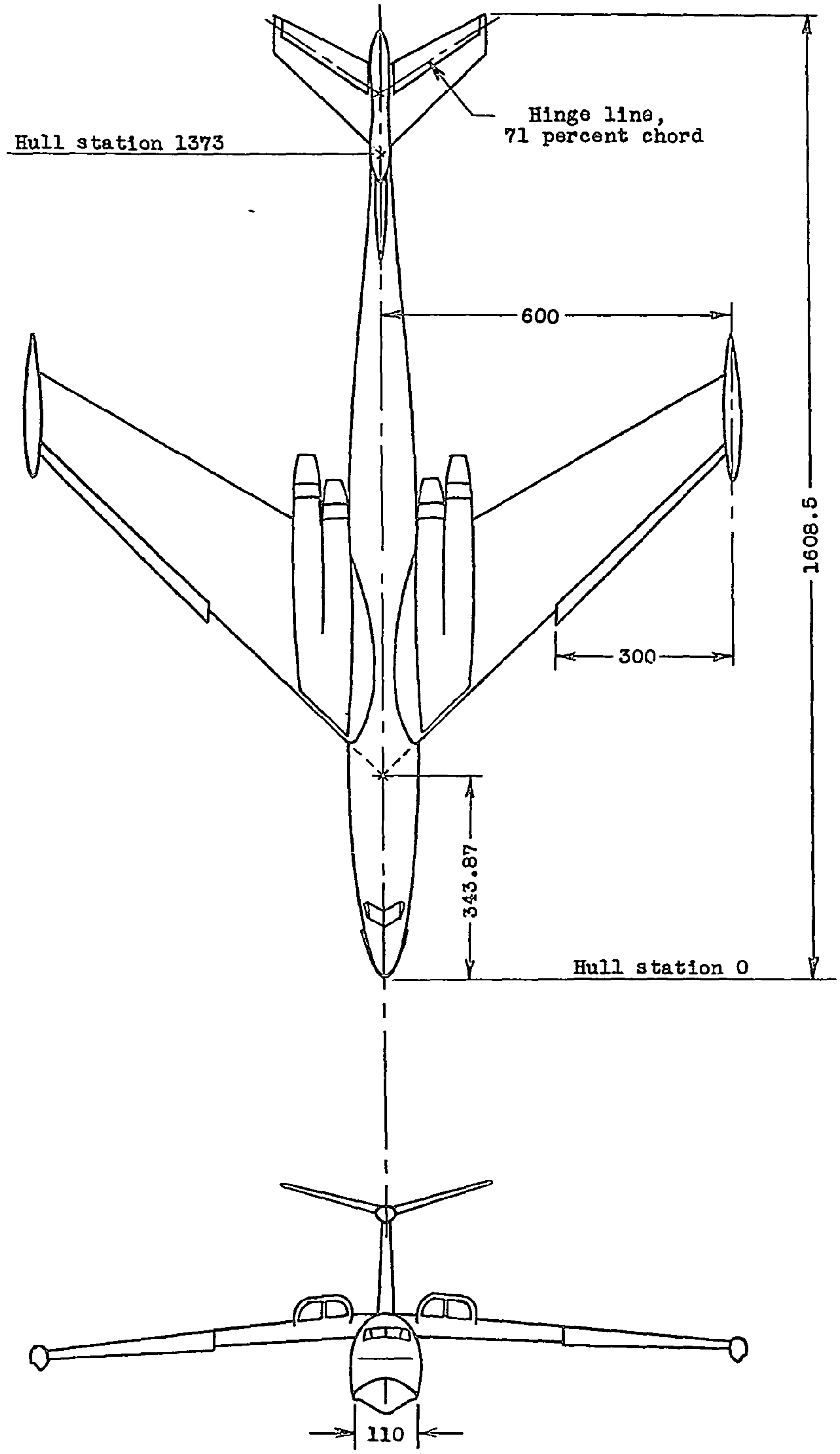

Figure 3.- General arrangement of the Martin XP6M-1 flying boat
(Dimensions are in inches, full size.)

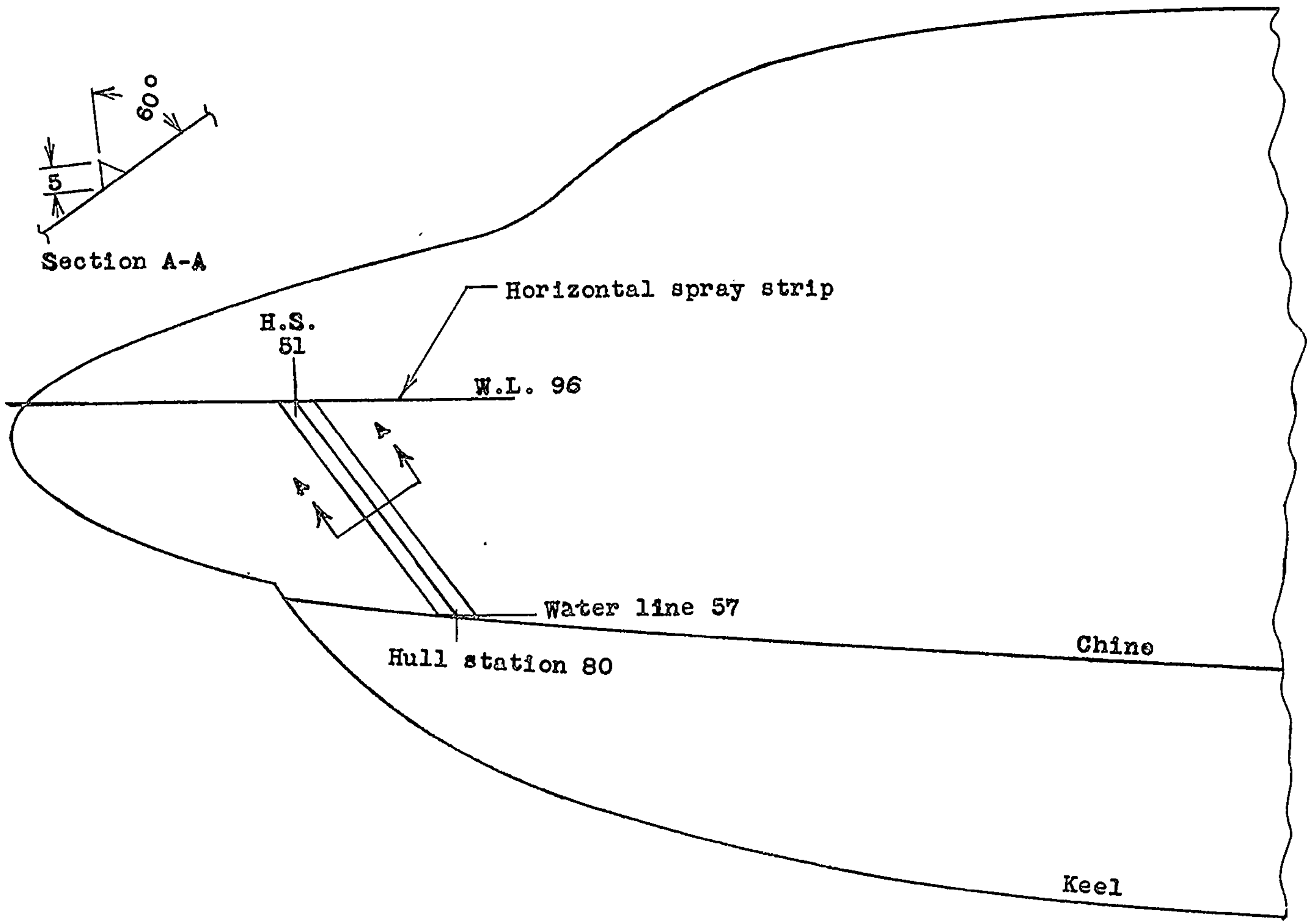

(a) Langley tank model 316-1.

Figure 4.- Spray-control devices used in bow region. (Dimensions are in inches.)

[redacted]

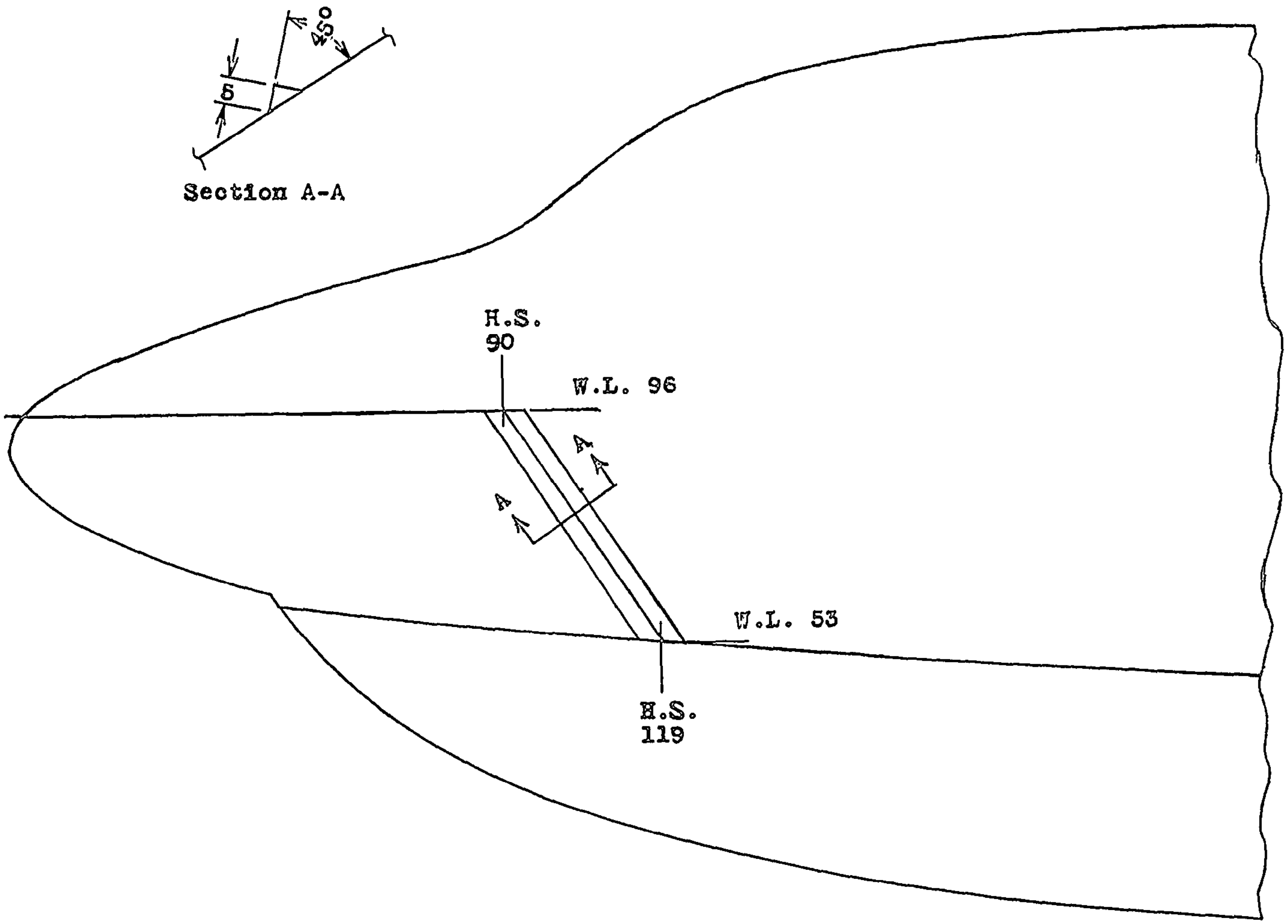

(b) Langley tank model 316-2.

Figure 4.- Continued.

[redacted]

[redacted]

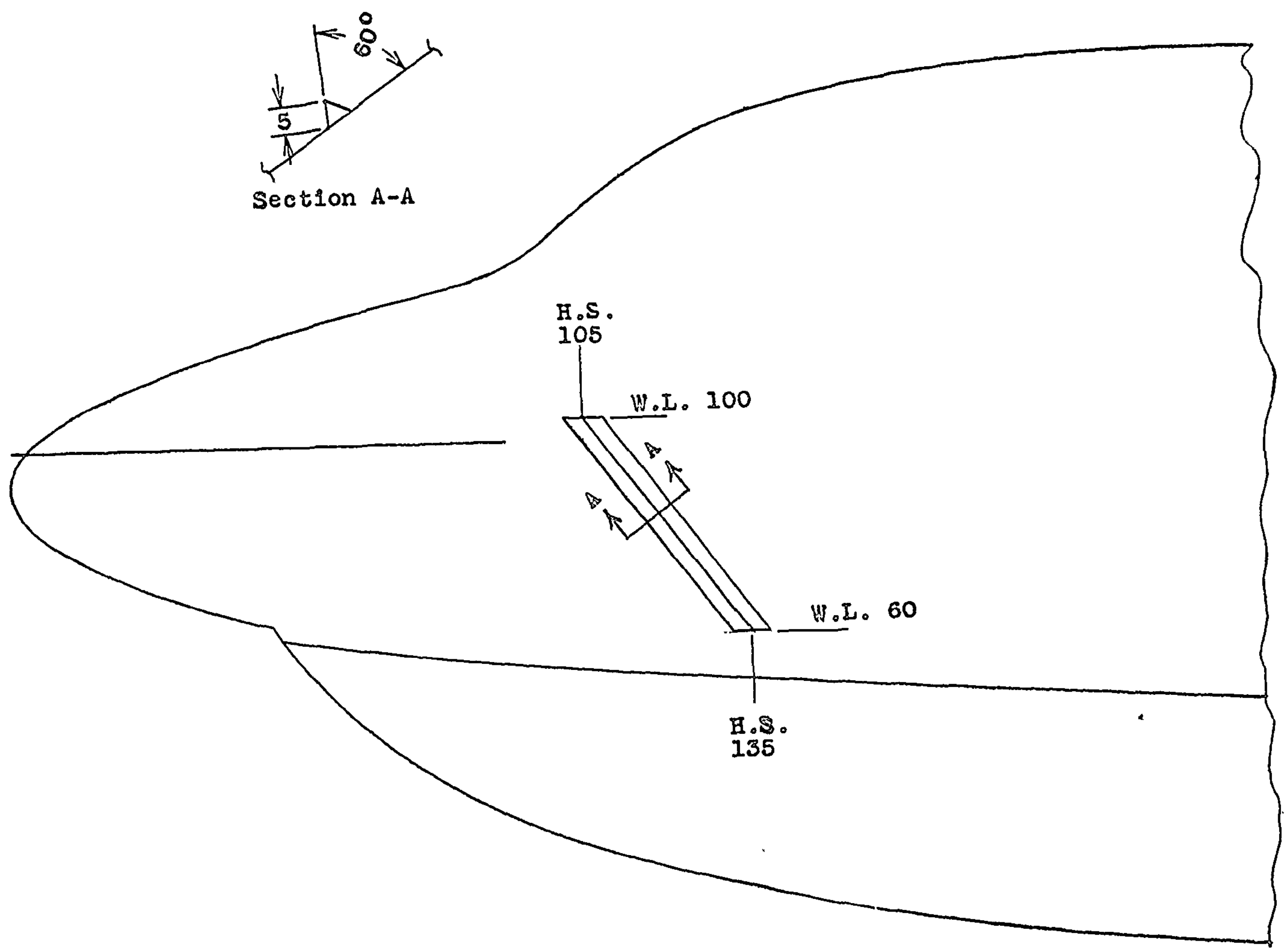

(c) Langley tank model 316-3.

Figure 4.- Continued.

[redacted]

[redacted]

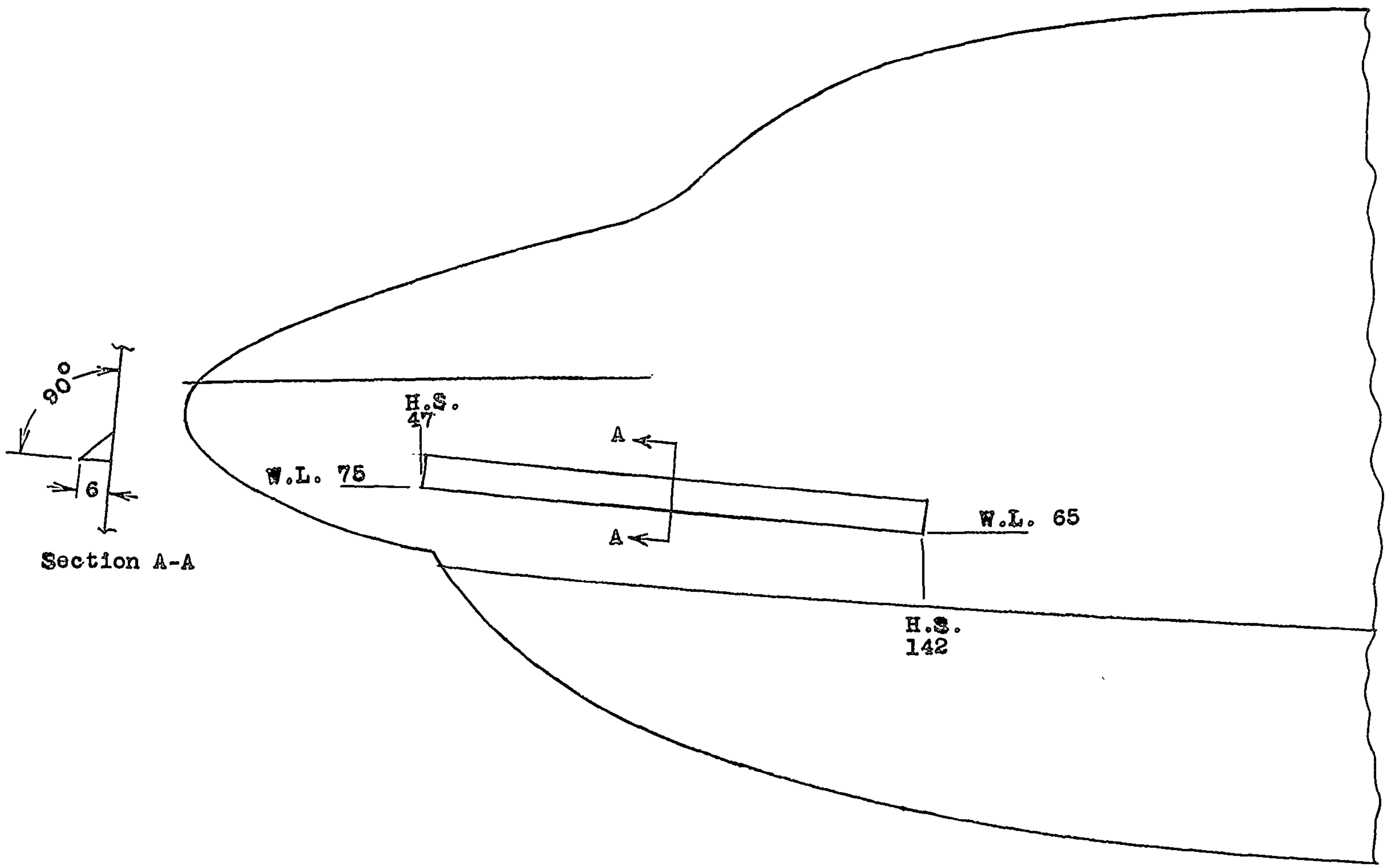

(d) Langley tank model 316-4.

Figure 4.- Continued.

[redacted]

[redacted]

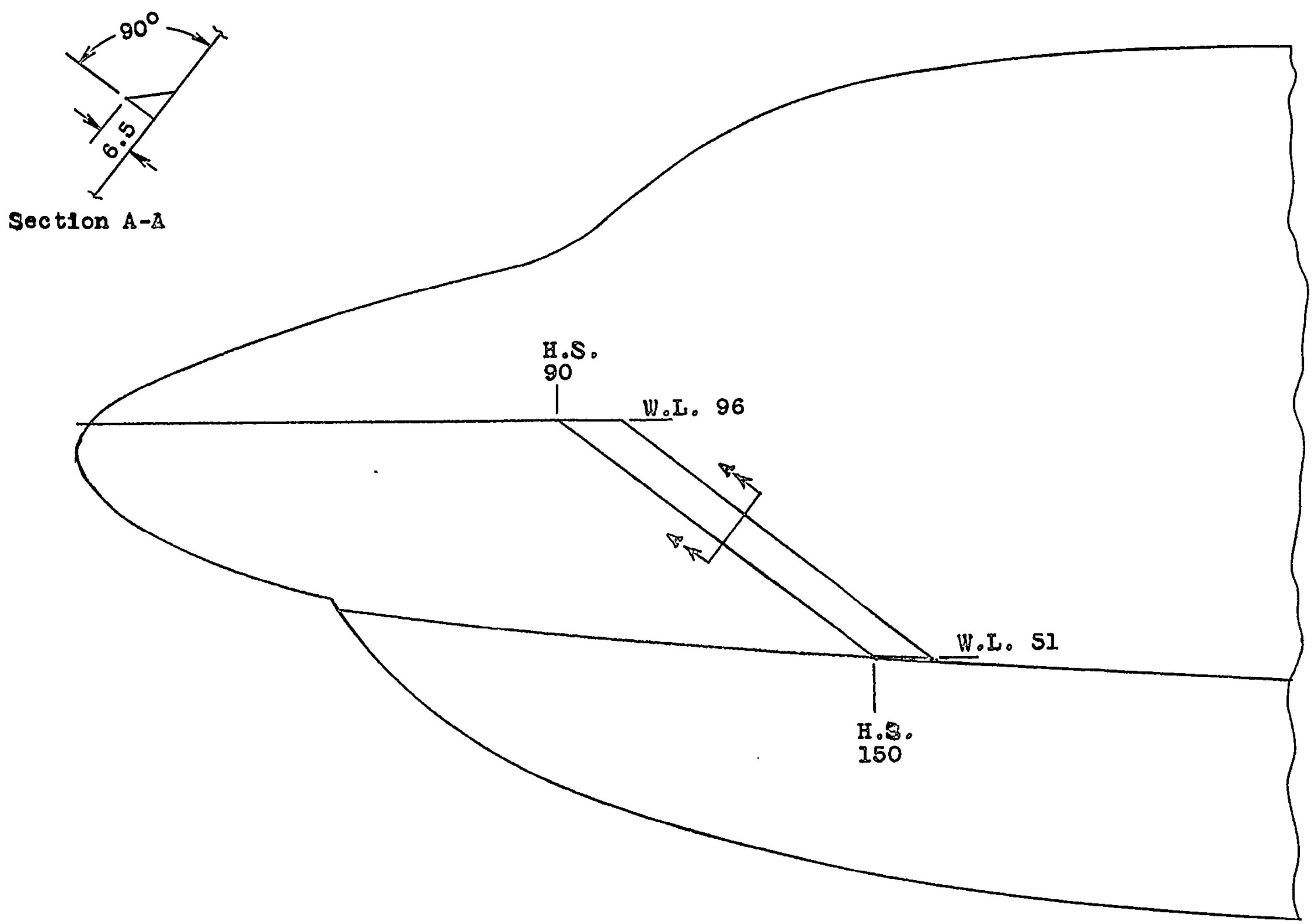

(e) Langley tank model 316-5.

Figure 4.- Continued.

[redacted]

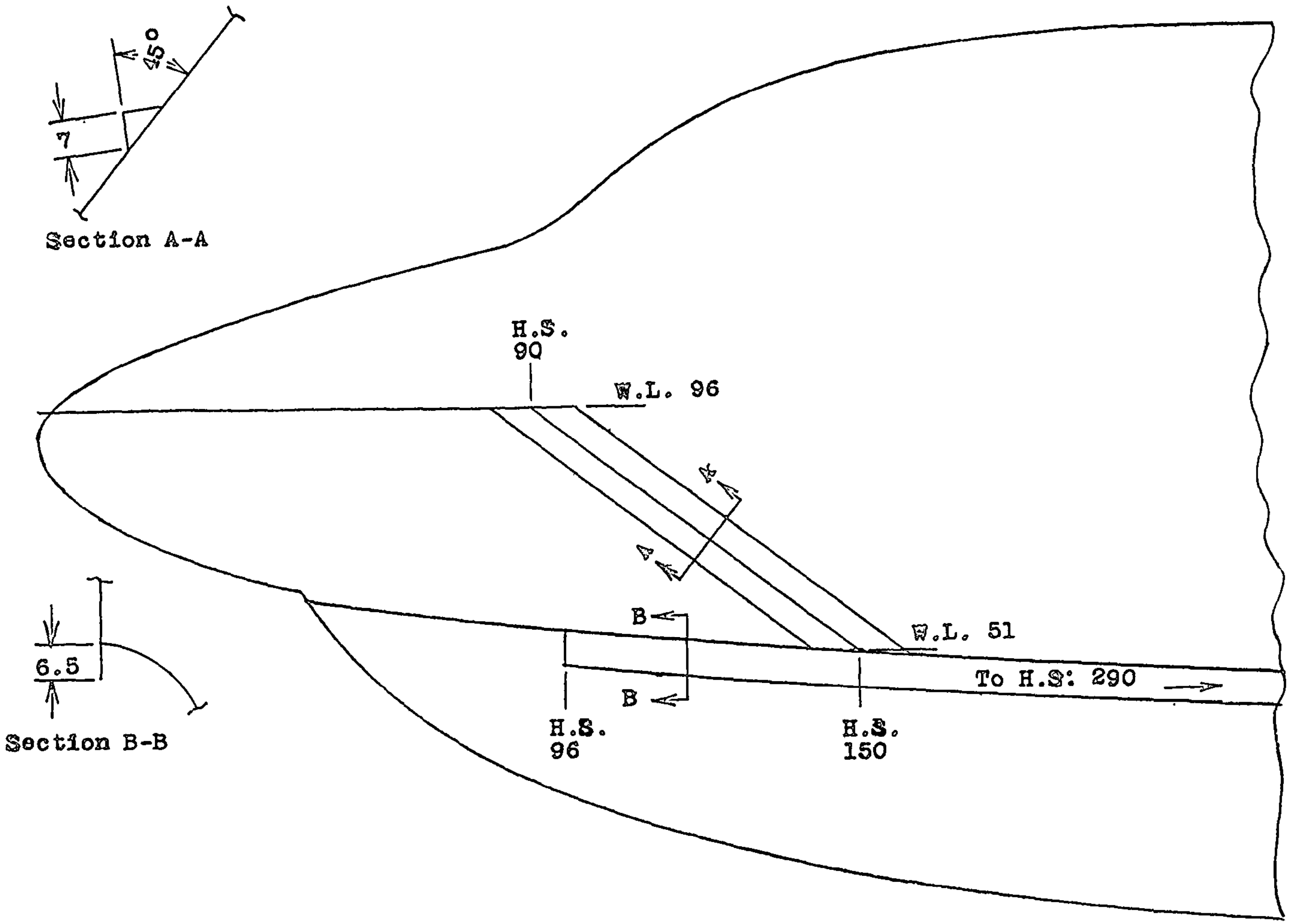

(f) Langley tank model 316-6.

Figure 4.- Continued.

[redacted]

[redacted]

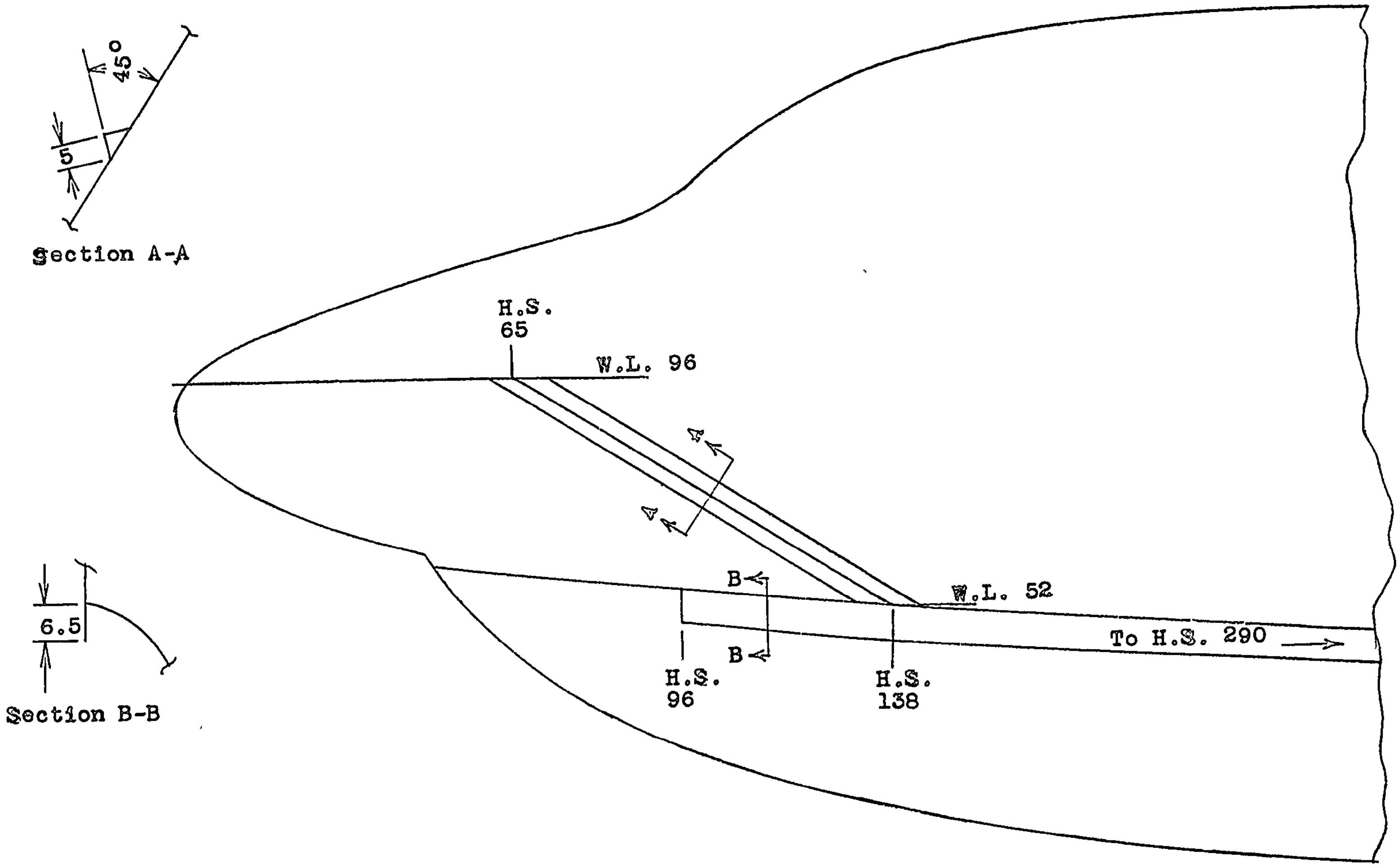

(g) Langley tank model 316-7.

Figure 4.- Continued.

[redacted]

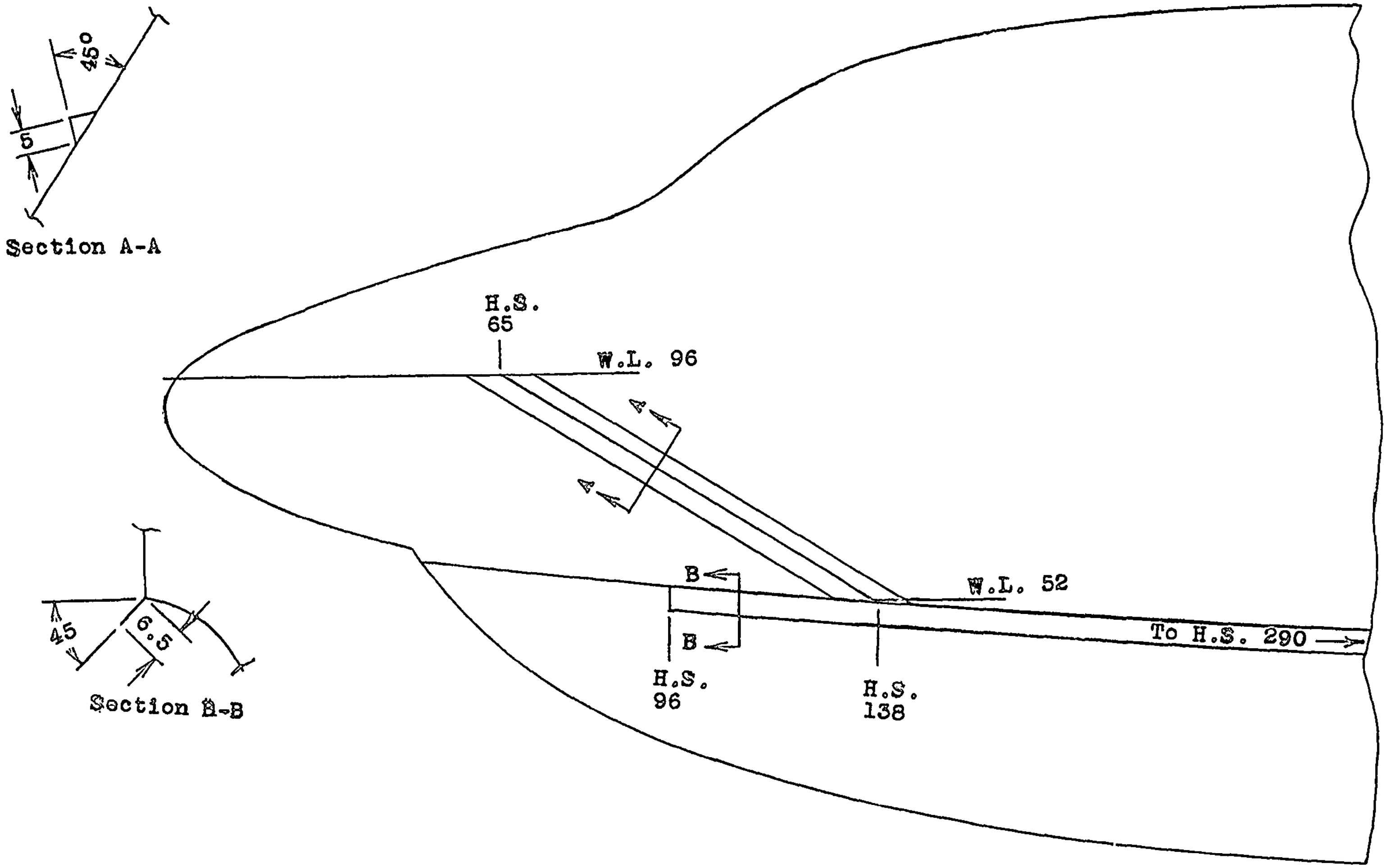

[redacted]

(h) Langley tank model 316-8.

Figure 4.- Continued.

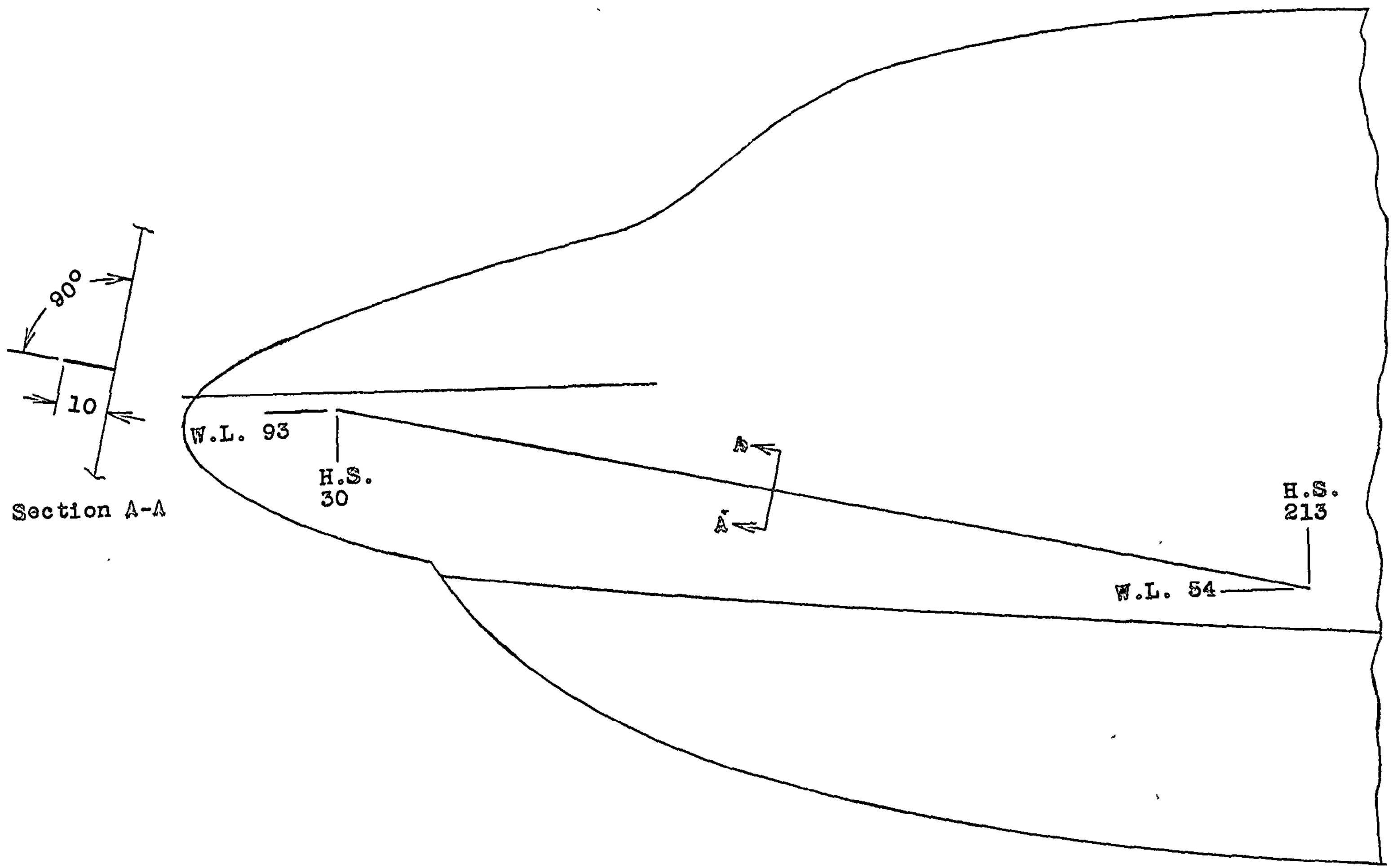

(i) Langley tank model 316-9.

Figure 4.- Continued.

[redacted]

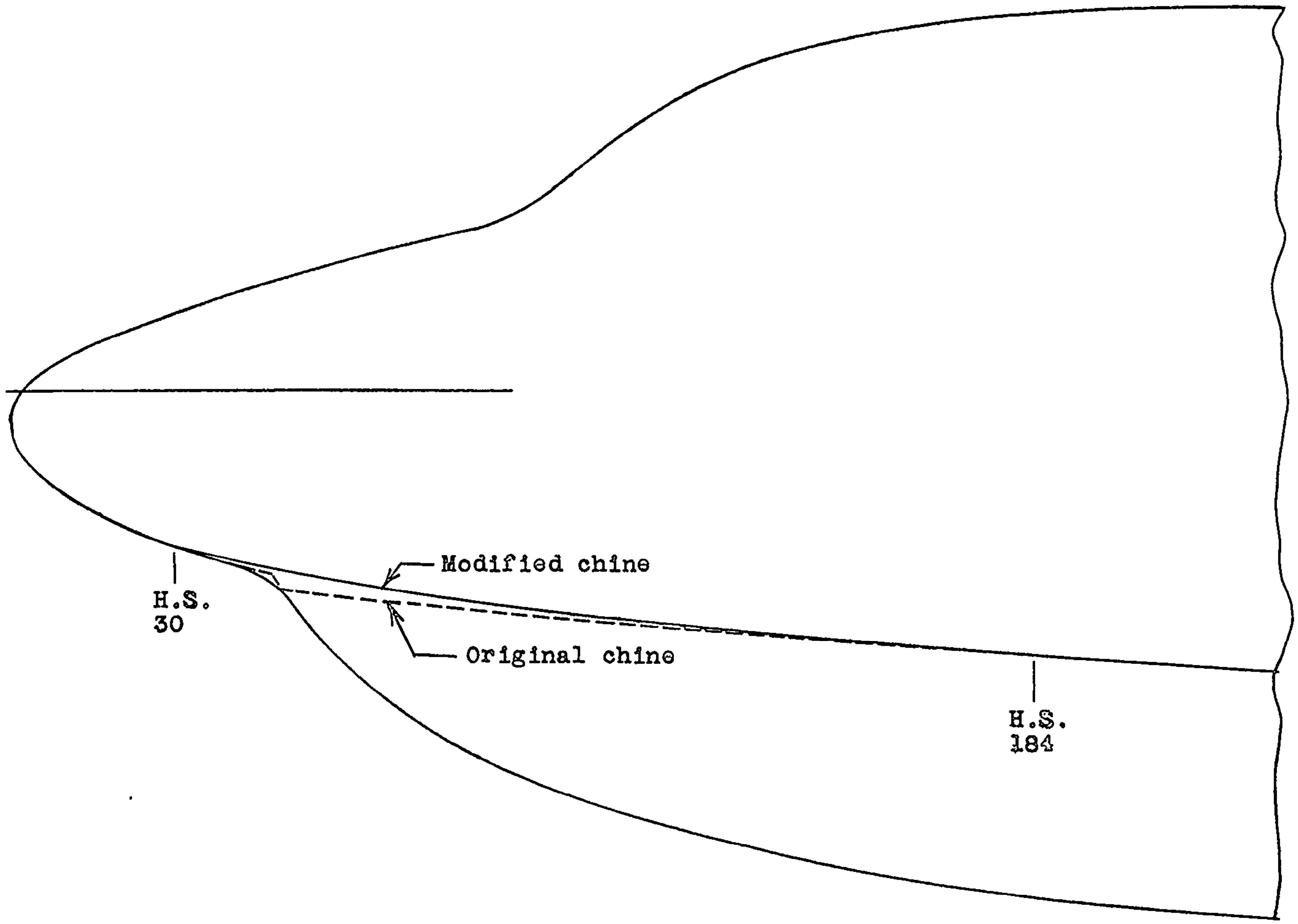

(j) Langley tank model 316-10.

Figure 4.- Continued.

[redacted]

[redacted]

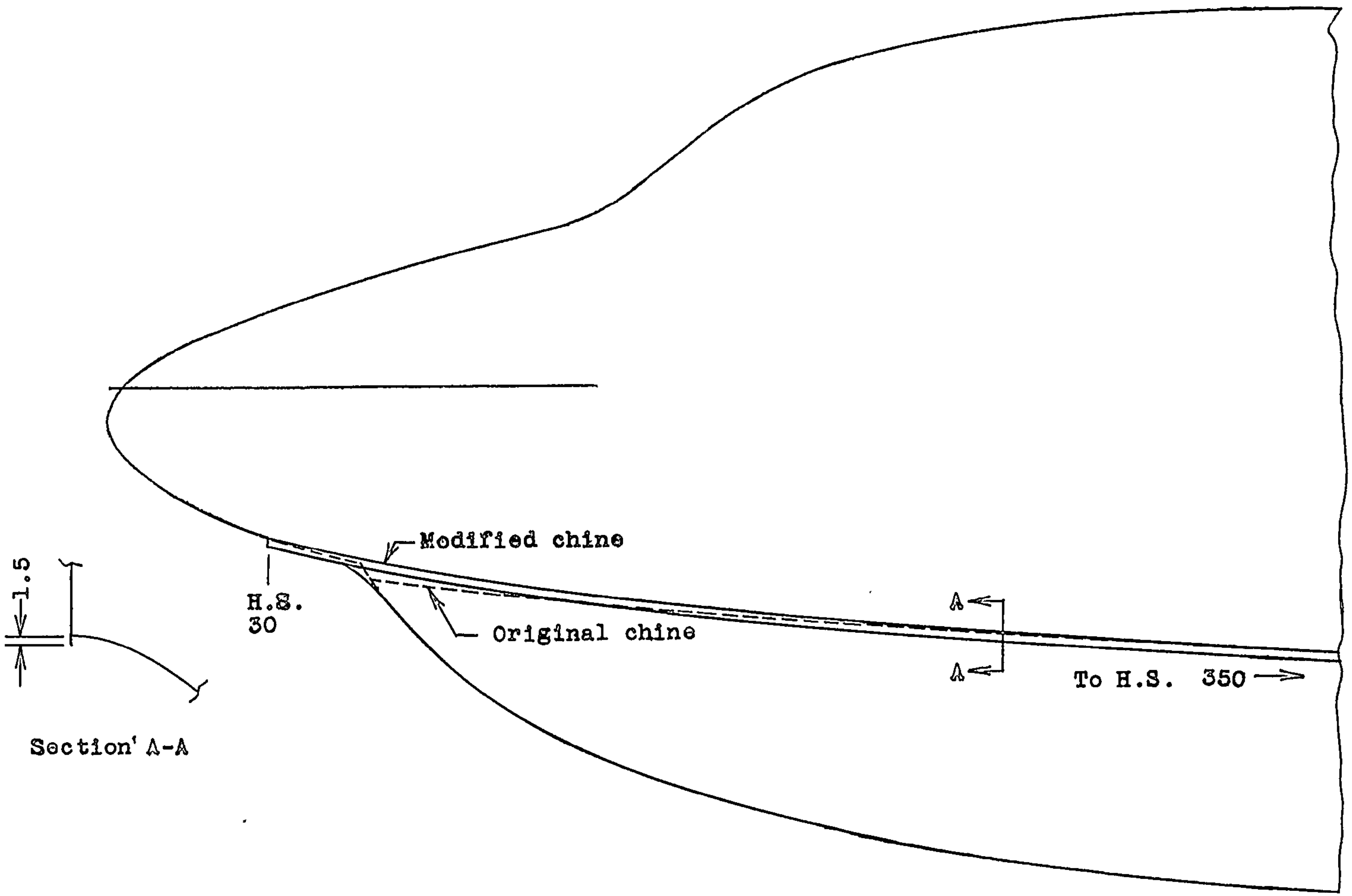

(k) Langley tank model 316-11.

Figure 4.- Concluded.

[redacted]

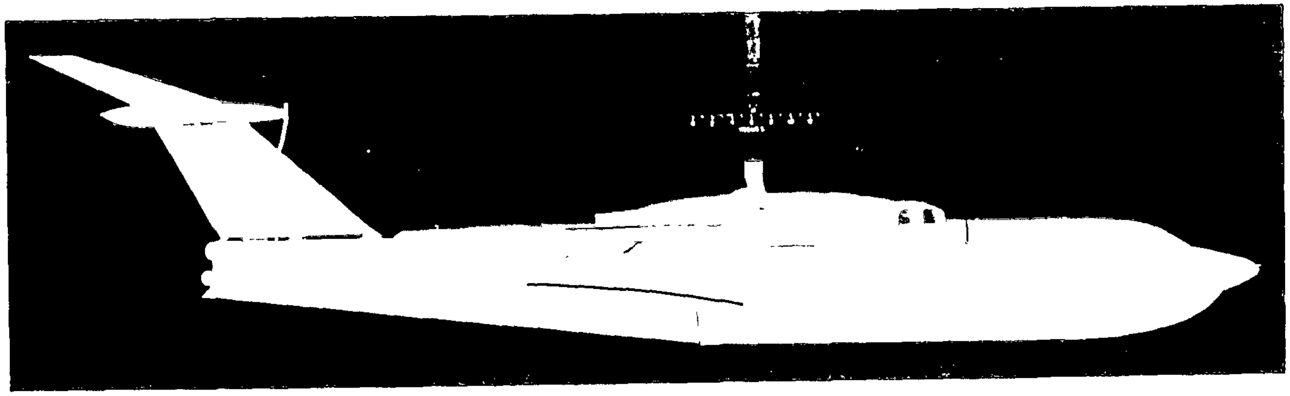

(a) Langley tank model 316-12.

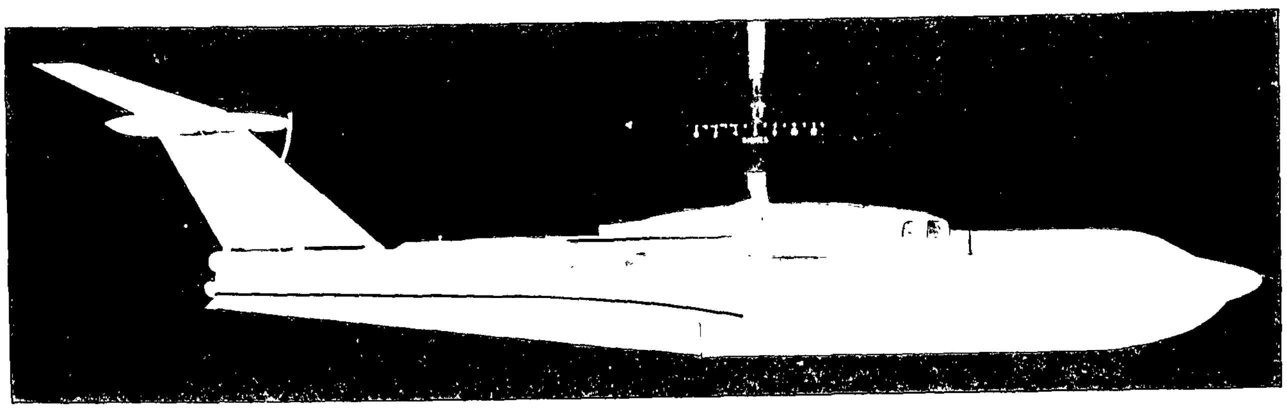

(b) Langley tank model 316-13.

L-87920

Figure 5.- Afterbody chine strips.

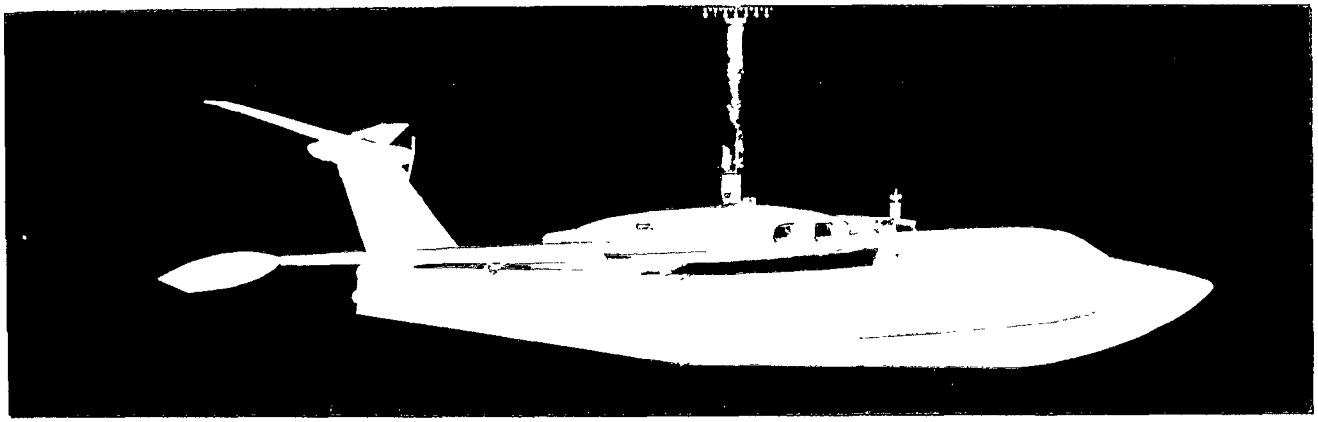

Three-quarter front view

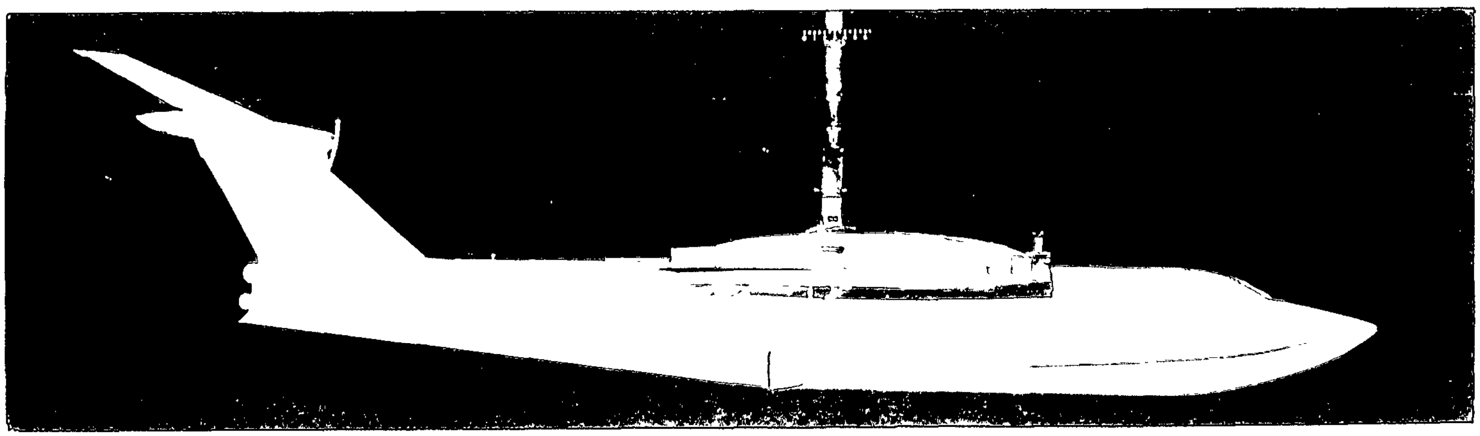

Profile view

L-87921

Figure 6.- Langley tank model 316A.

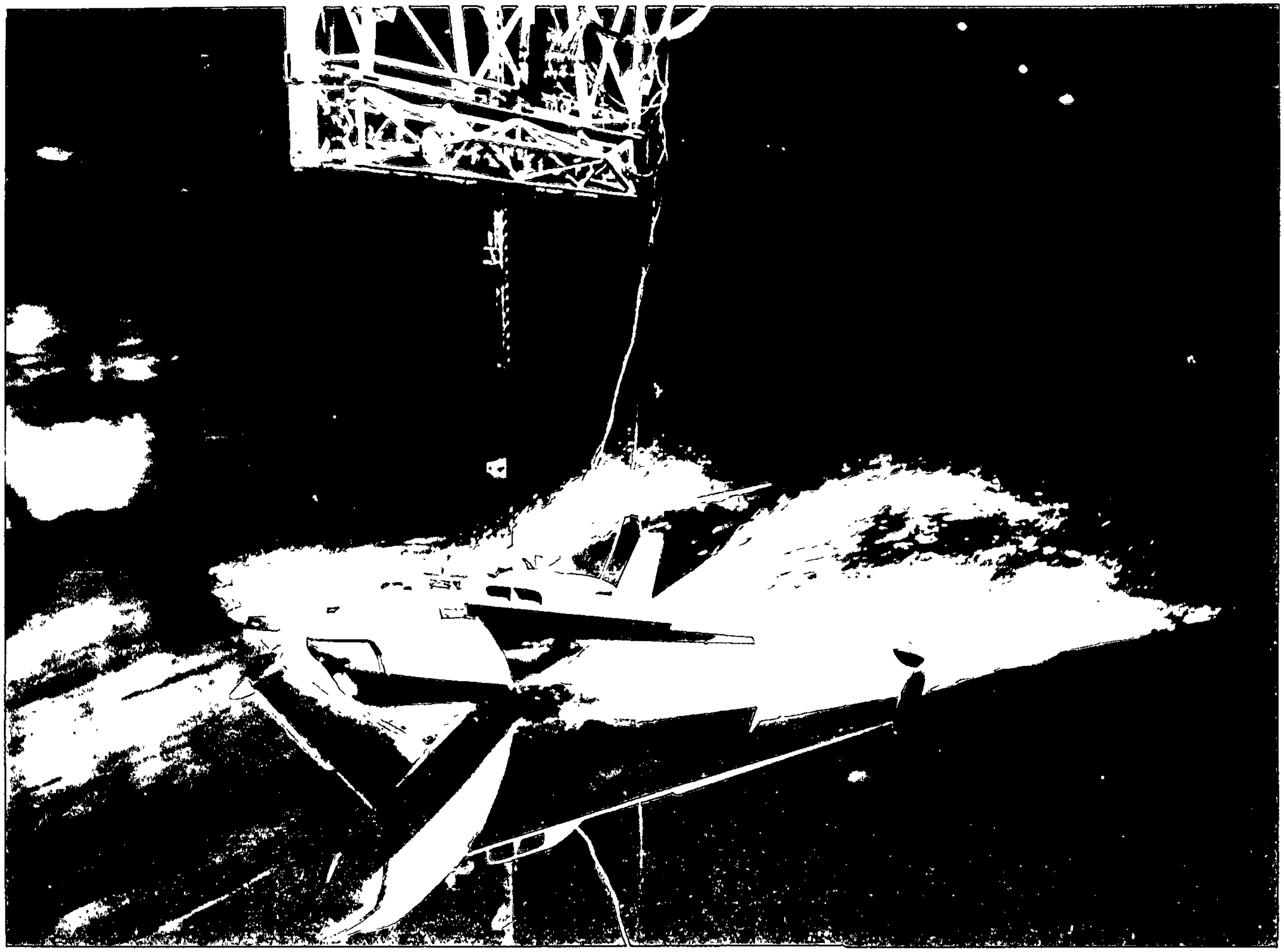

L-88142

Figure 7.- Setup of Langley tank model 316-5 on towing apparatus.

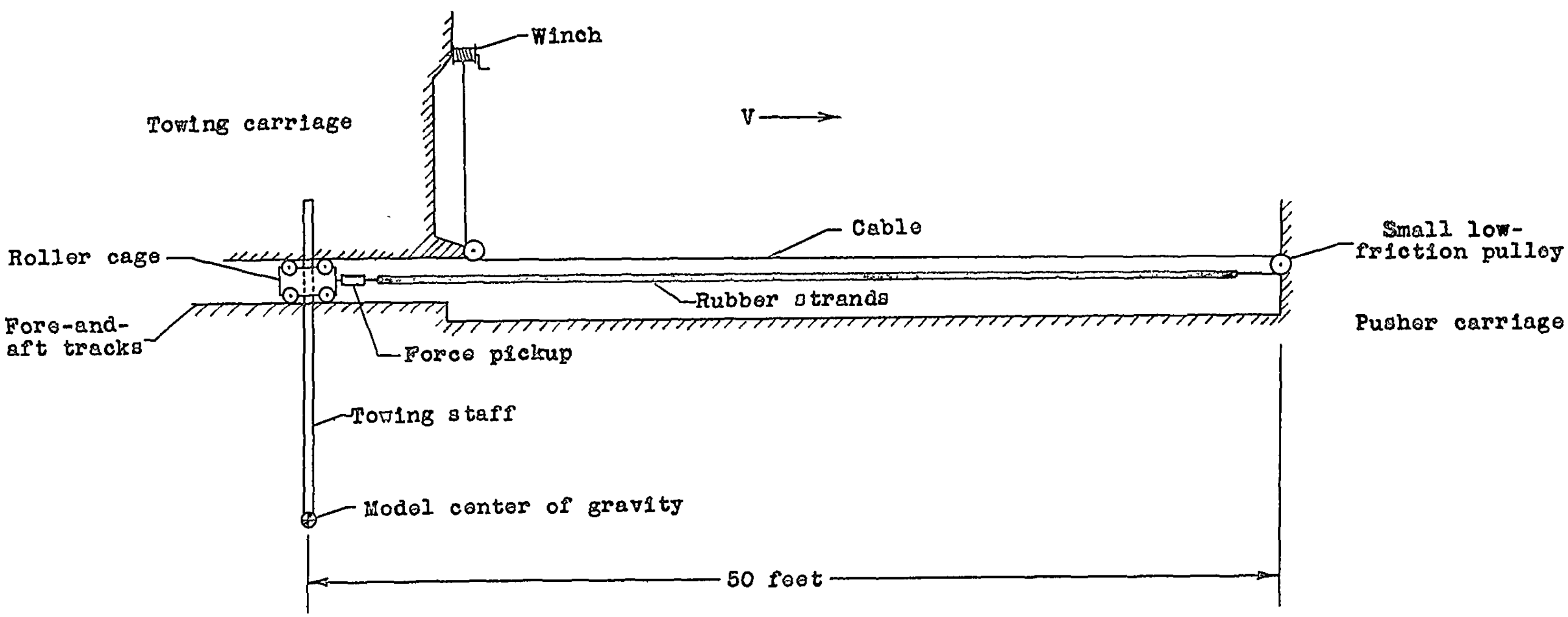

Figure 8.- Schematic diagram of setup used to determine resistance in rough water.

L-84601.1

Figure 9.- Setup of Langley tank model 316A on apparatus for launching as a free body.

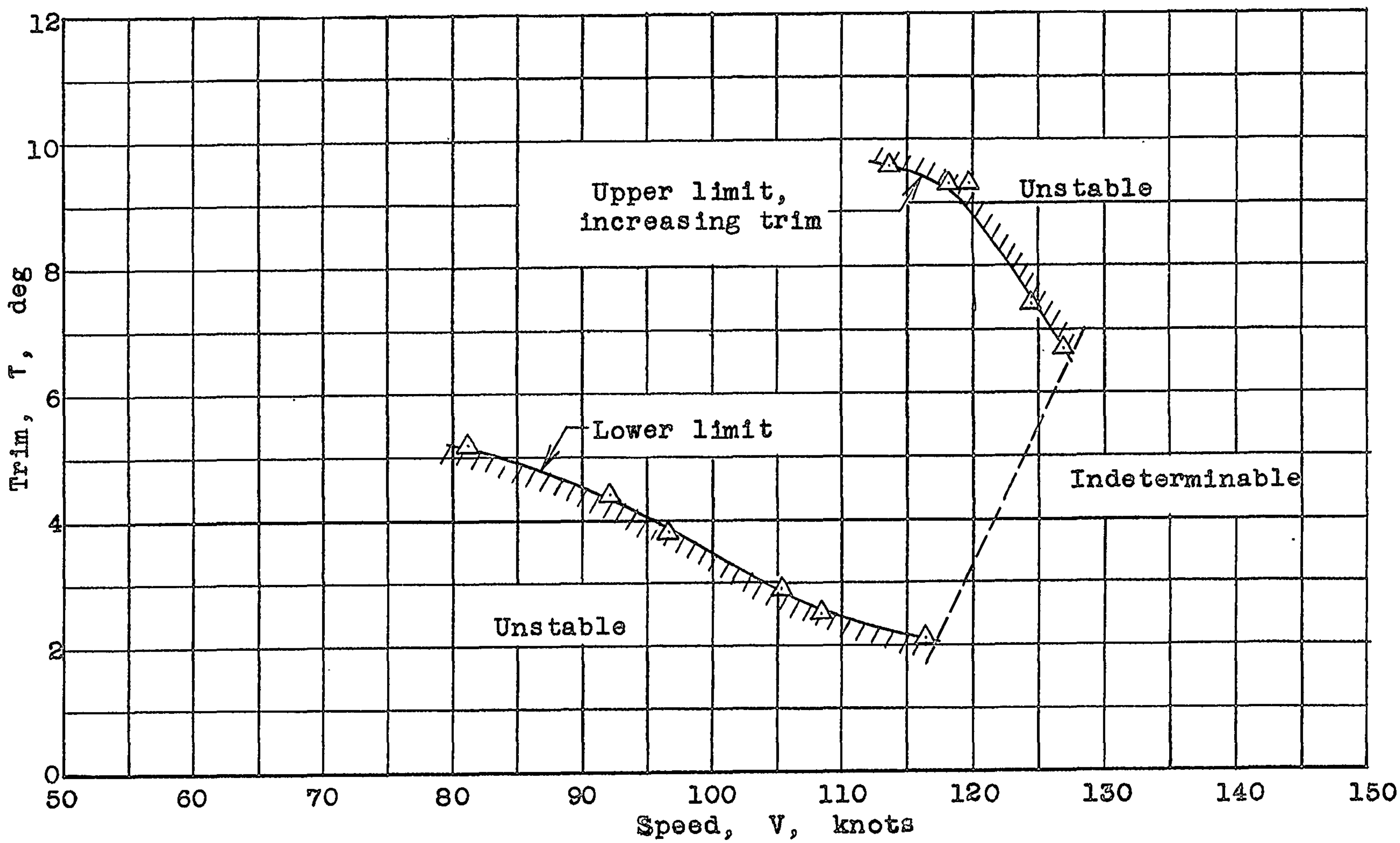

Figure 10.- Trim limits of stability. Δ_0 = 160,000 pounds; $\delta_f = 40^\circ$; power off. Langley tank model 316.

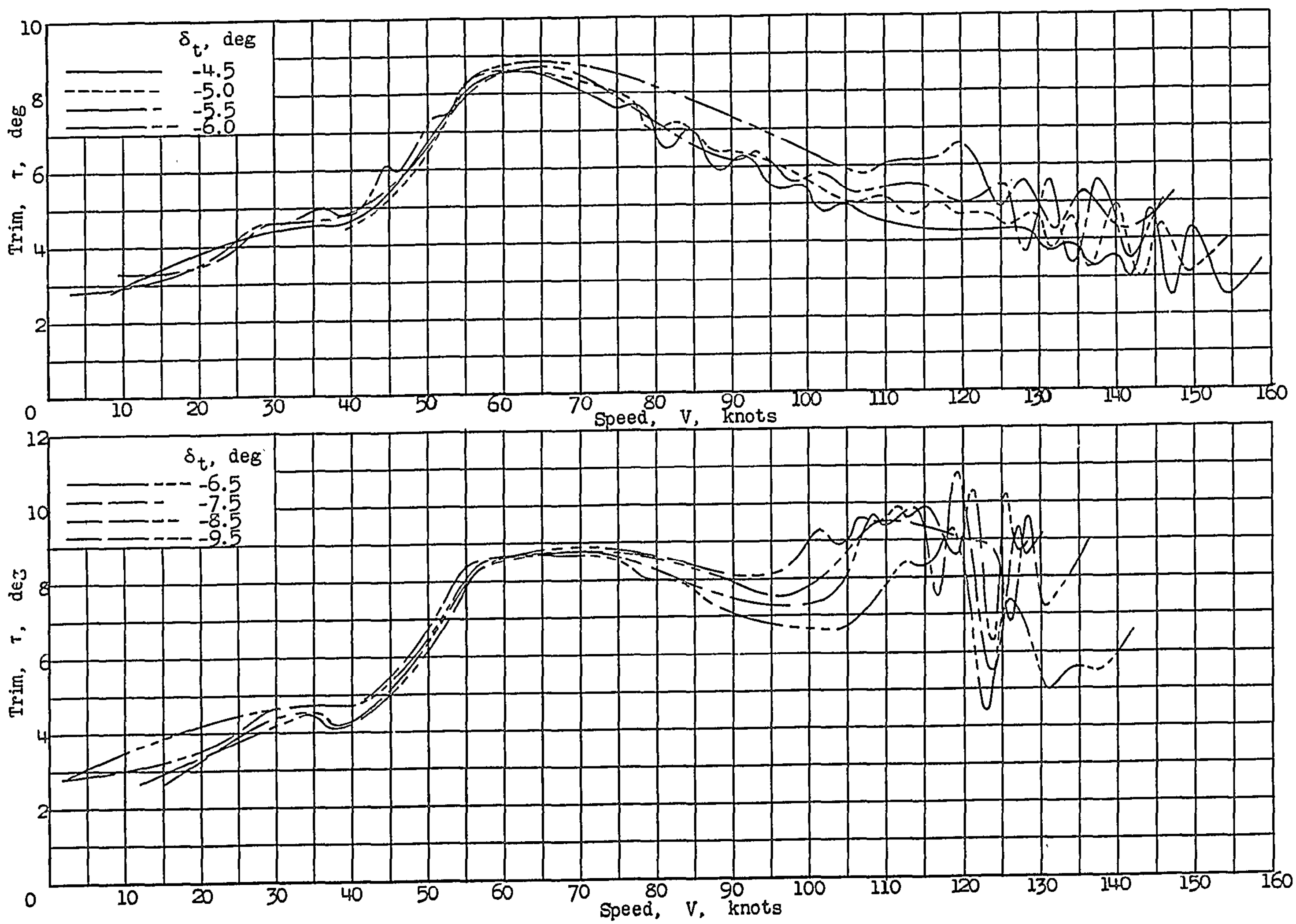

Figure 11.- Variation of trim with speed during take-off. Δ_o = 160,000 pounds; δ_f = 40°; power on. Langley tank model 316.

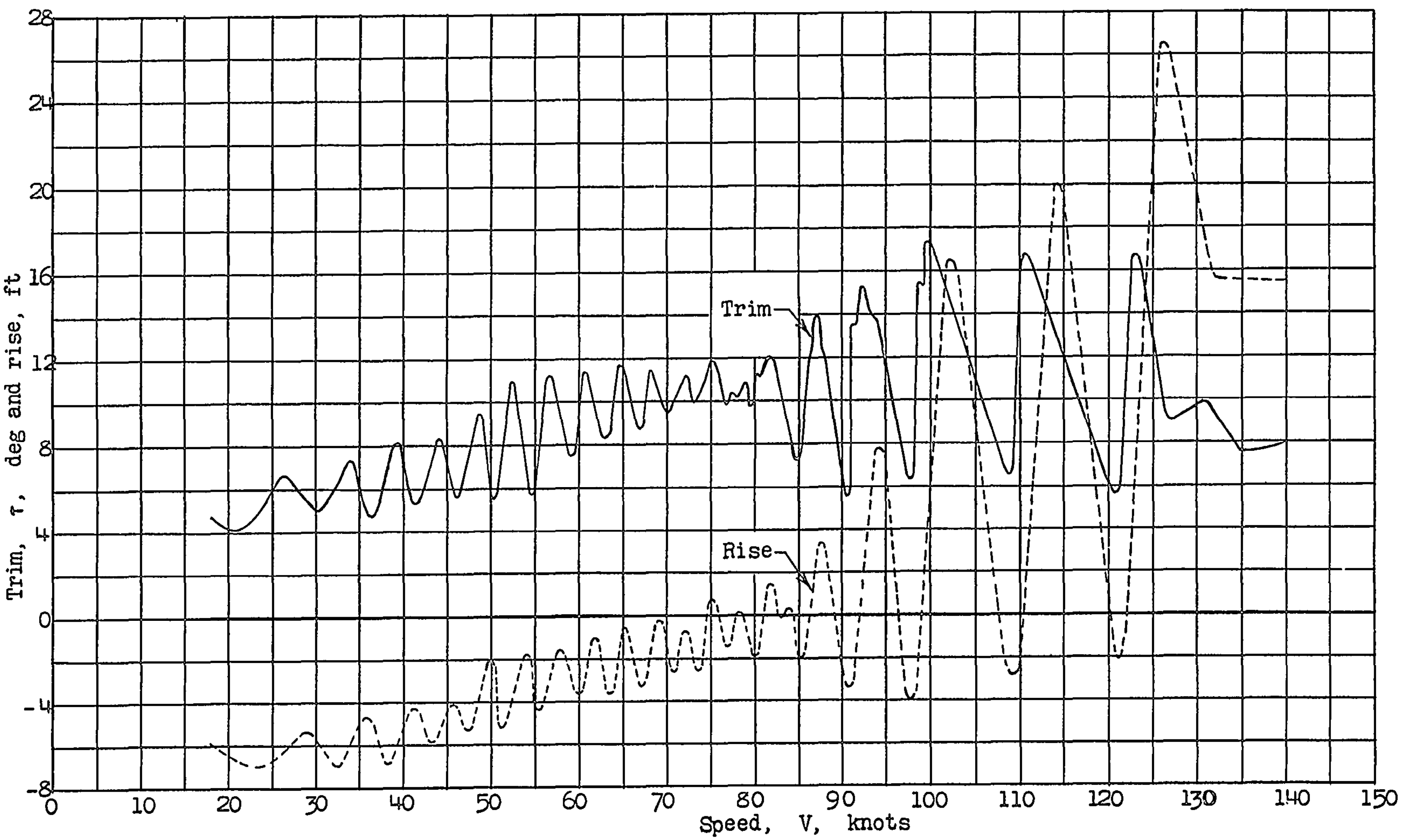

Figure 12.- Variation of trim and rise with speed during typical take-off in 4-foot waves. Δ_o = 160,000 pounds; δ_f = 40°; power on. Langley tank model 316A.

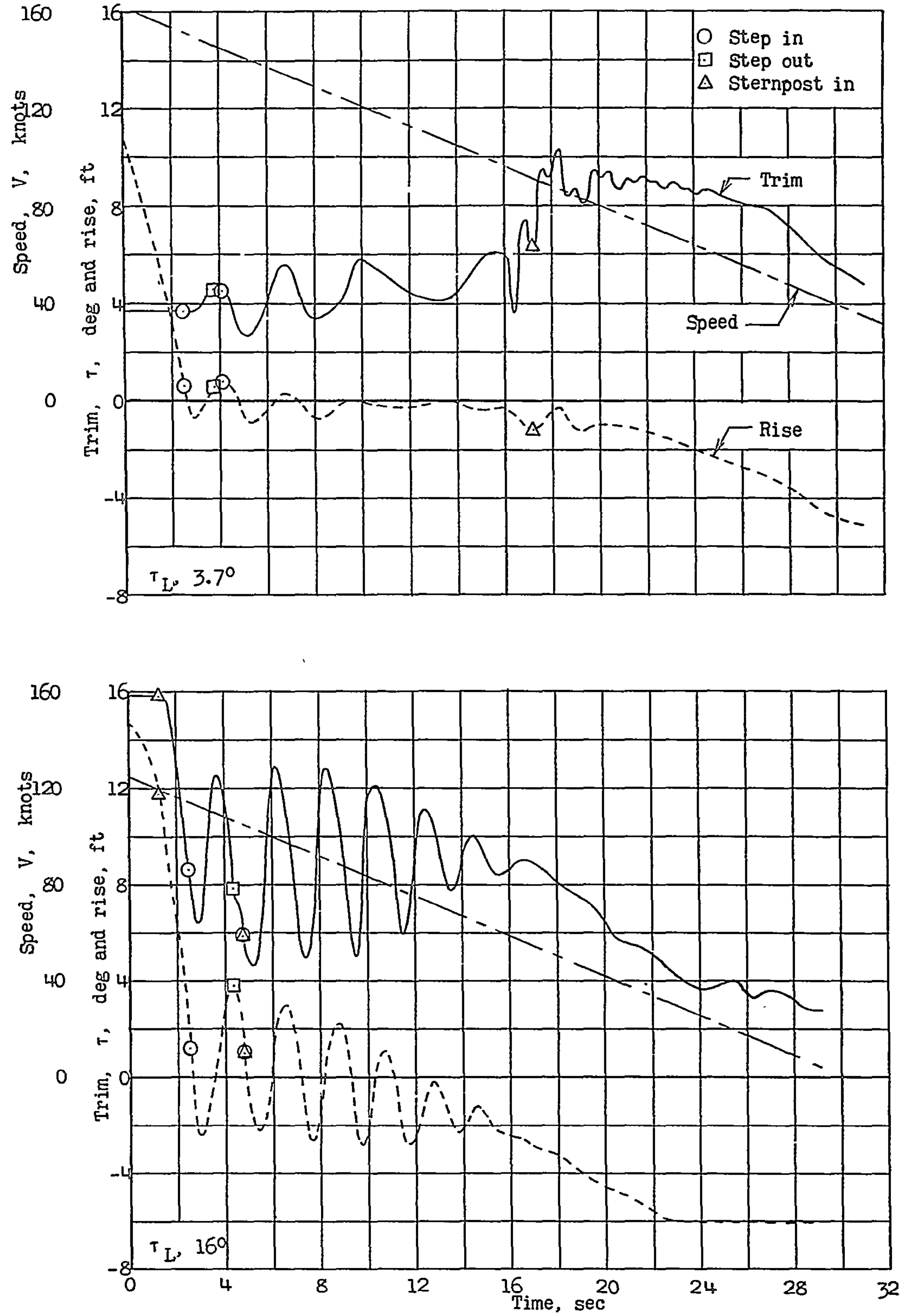

Figure 13.- Variation of trim, rise, and speed with time during typical landings in smooth water. Δ_o = 160,000 pounds; δ_f = 40°; power off. Langley tank model 316.

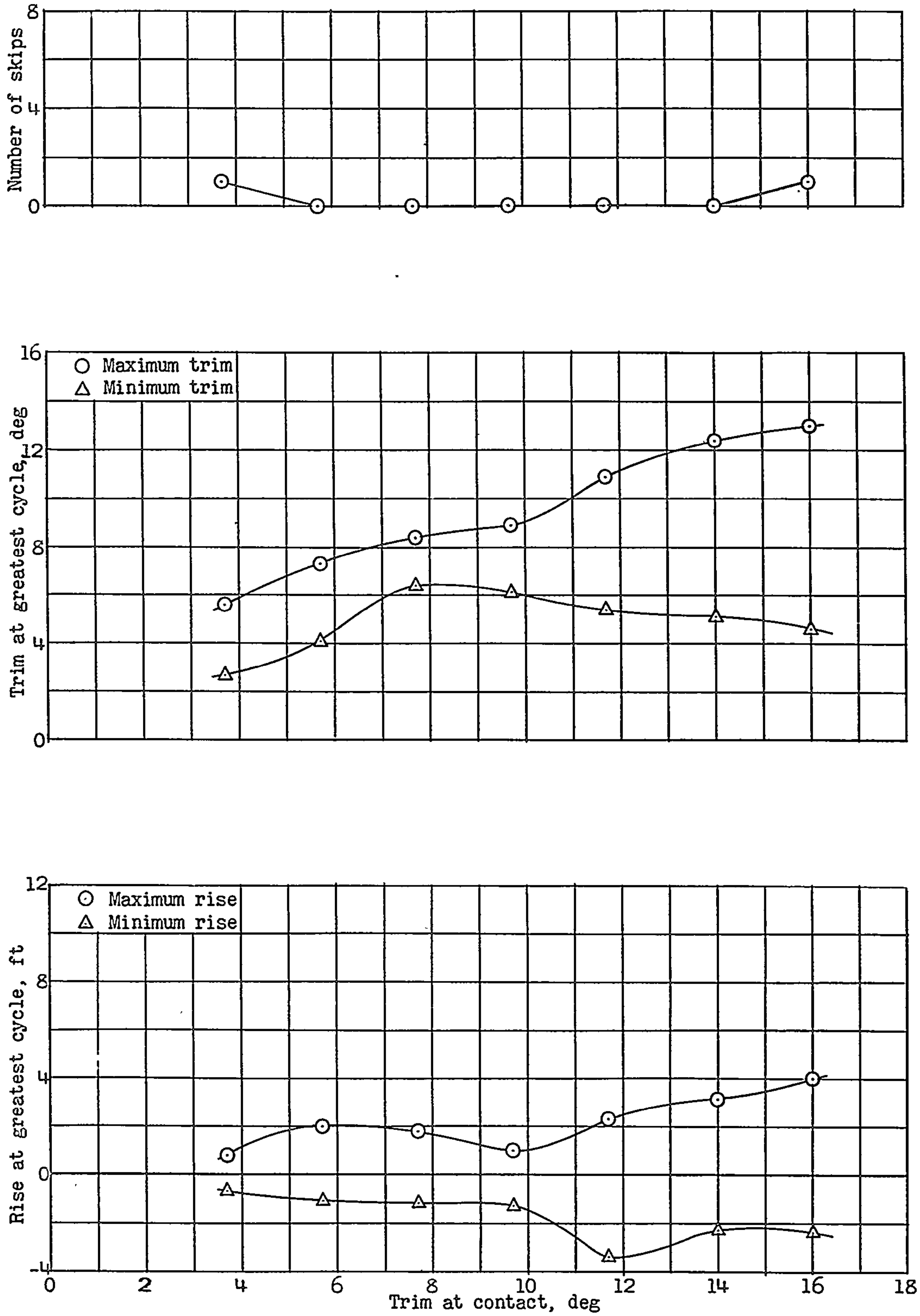

Figure 14.- Landing stability characteristics in smooth water. Δ_o = 160,000 pounds; δ_f = 40°; power off. Langley tank model 316.

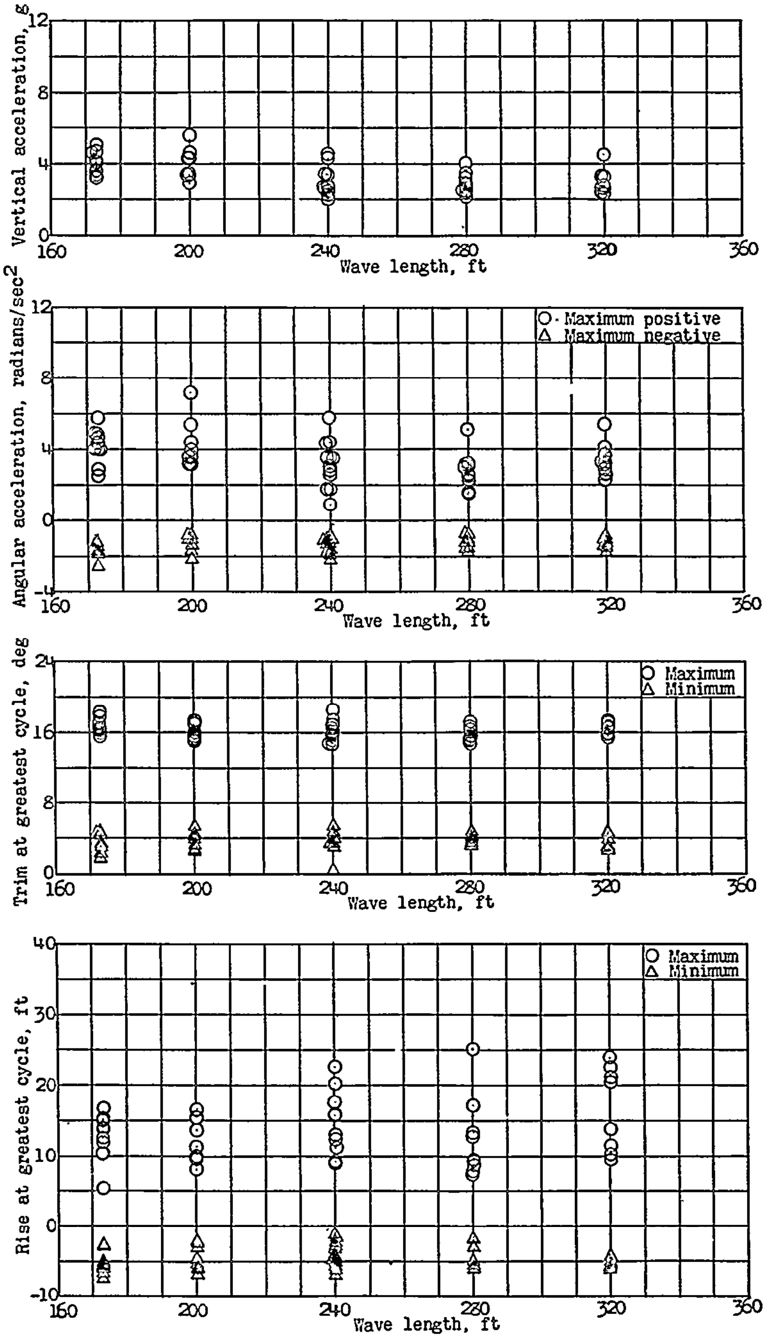

(a) Wave height, 4 feet.

Figure 15.- Effect of wave length on rough-water landing characteristics. Δ_o = 160,000 pounds; $\delta_f = 40^\circ$; $\delta_t = -7\frac{1}{2}^\circ$; $\tau_L = 12^\circ$; power off. Langley tank model 316.

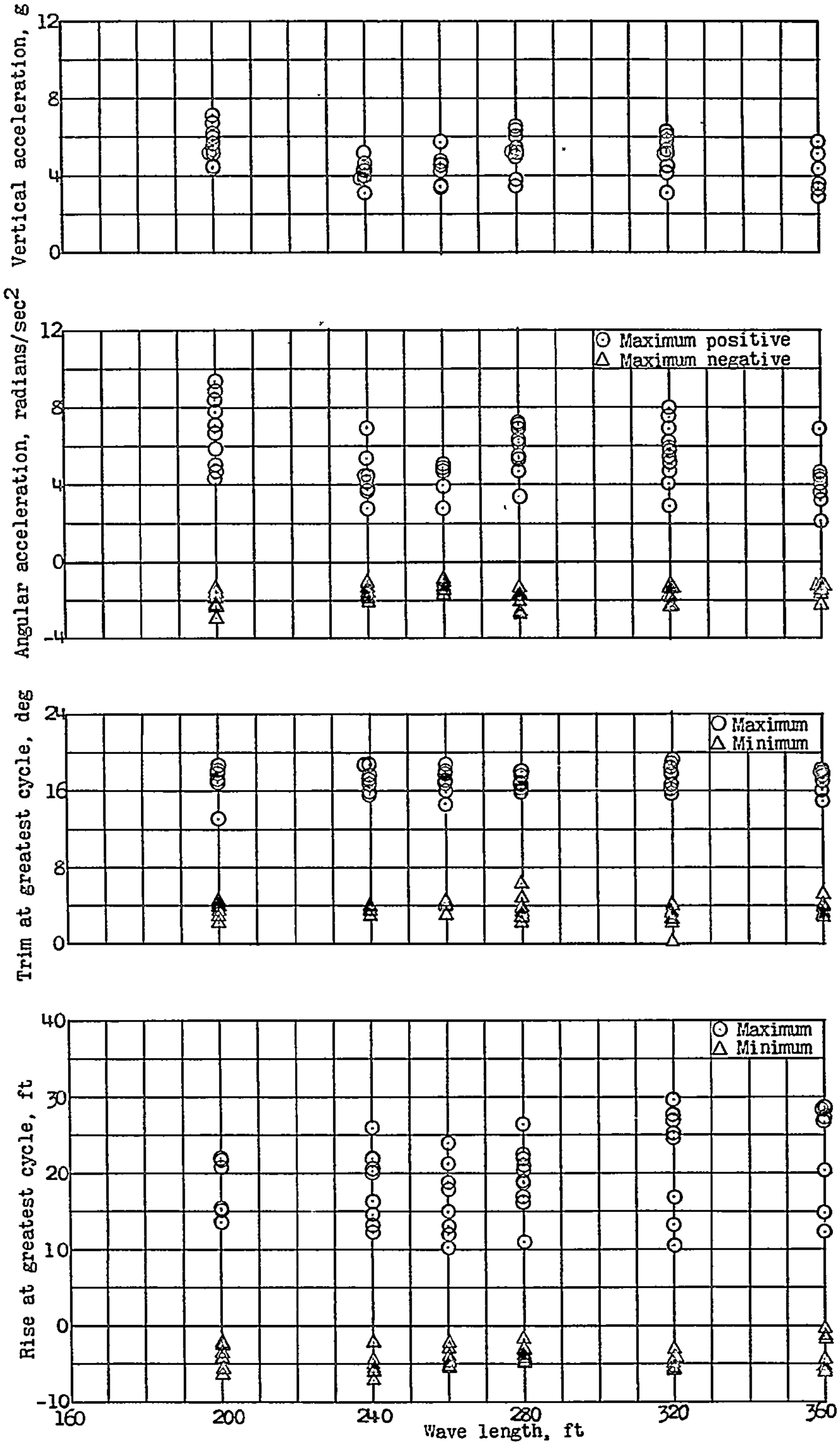

(b) Wave height, 6 feet.

Figure 15.- Continued.

[redacted]

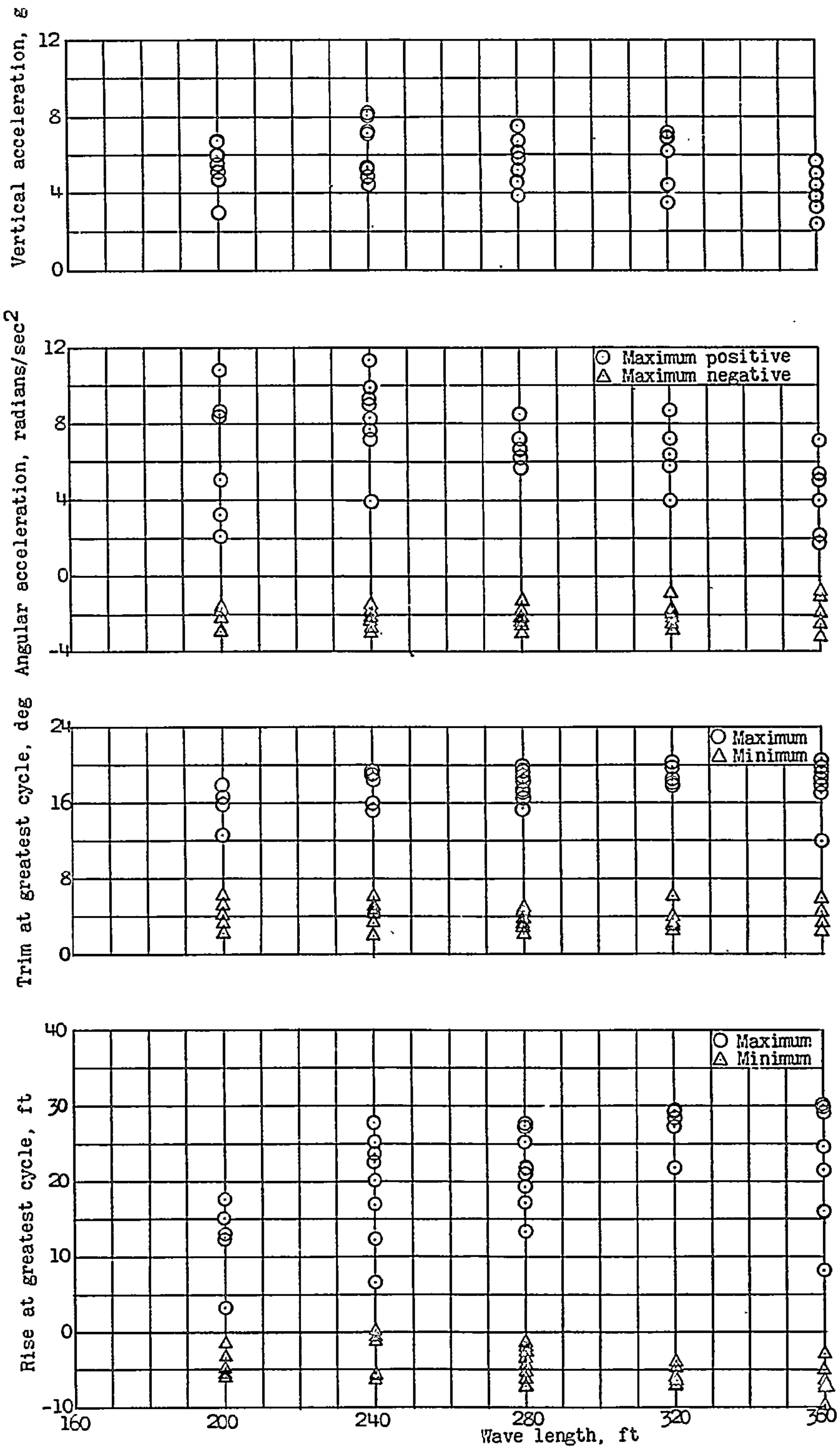

(c) Wave height, 8 feet.

Figure 15.- Concluded.

[redacted]

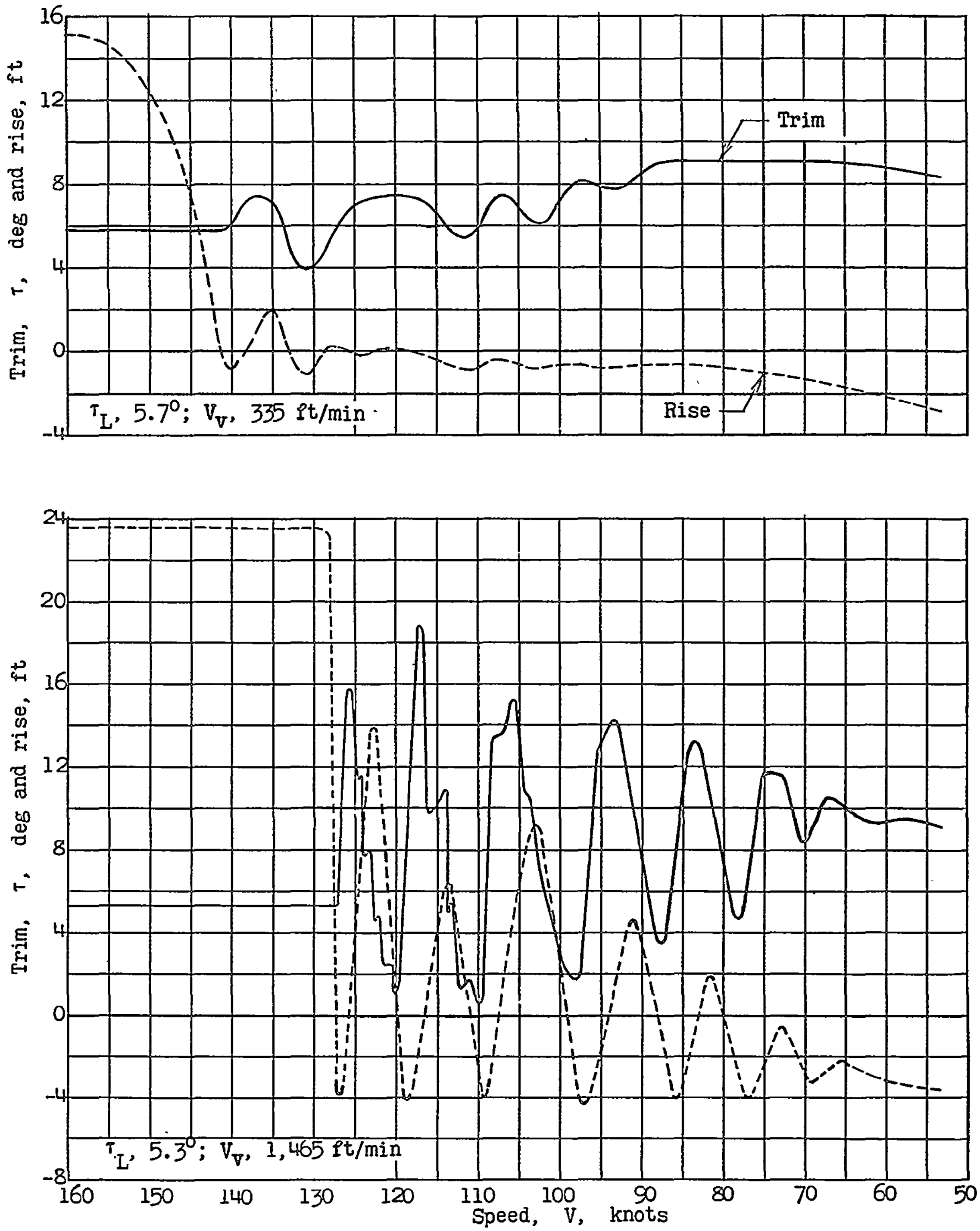

(a) Smooth water.

Figure 16.- Effect of high sinking speed on landing behavior. Δ_o = 160,000 pounds; δ_f = 40°; power off. Langley tank model 316.

[redacted]

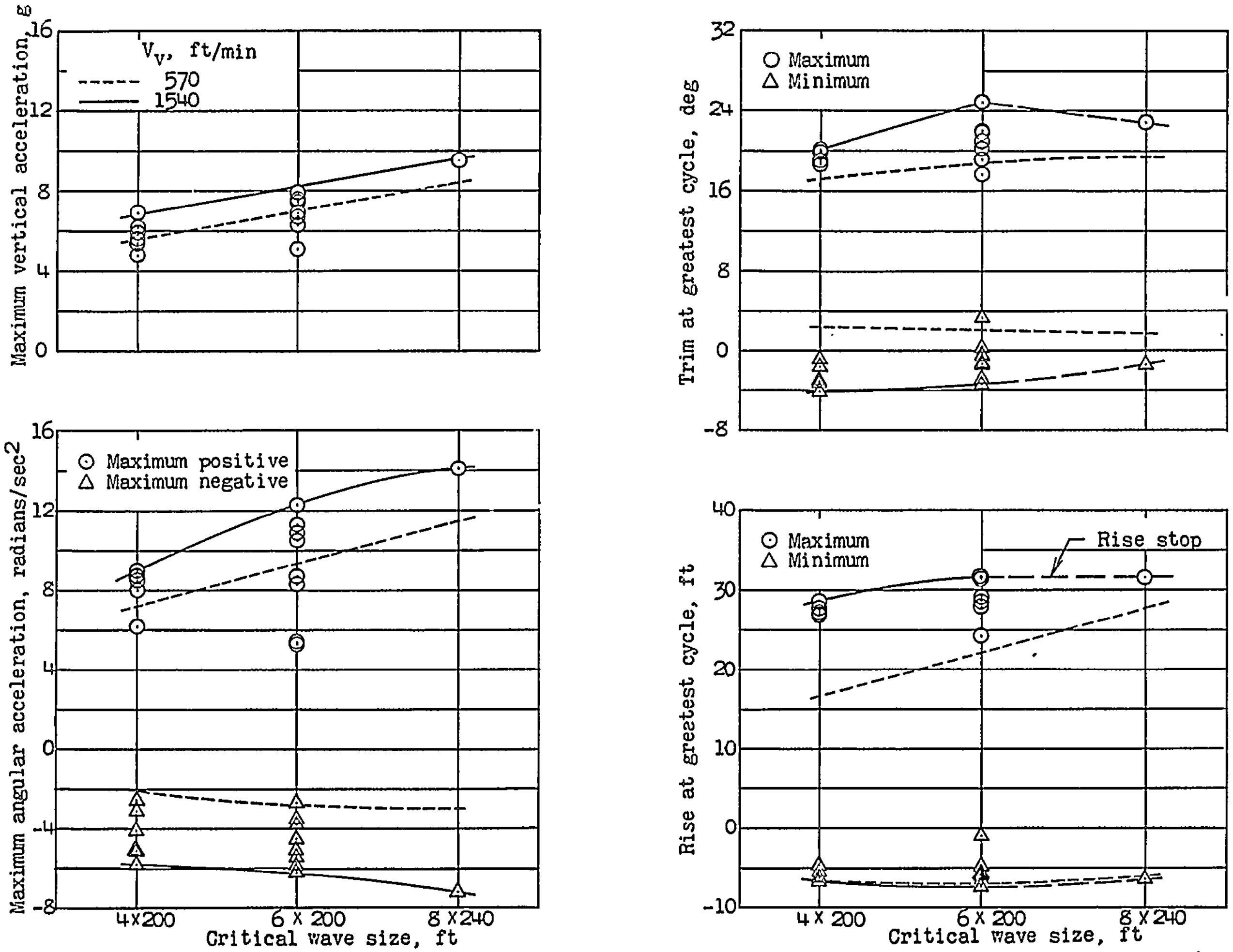

(b) Rough water.

Figure 16.- Concluded.

[redacted]

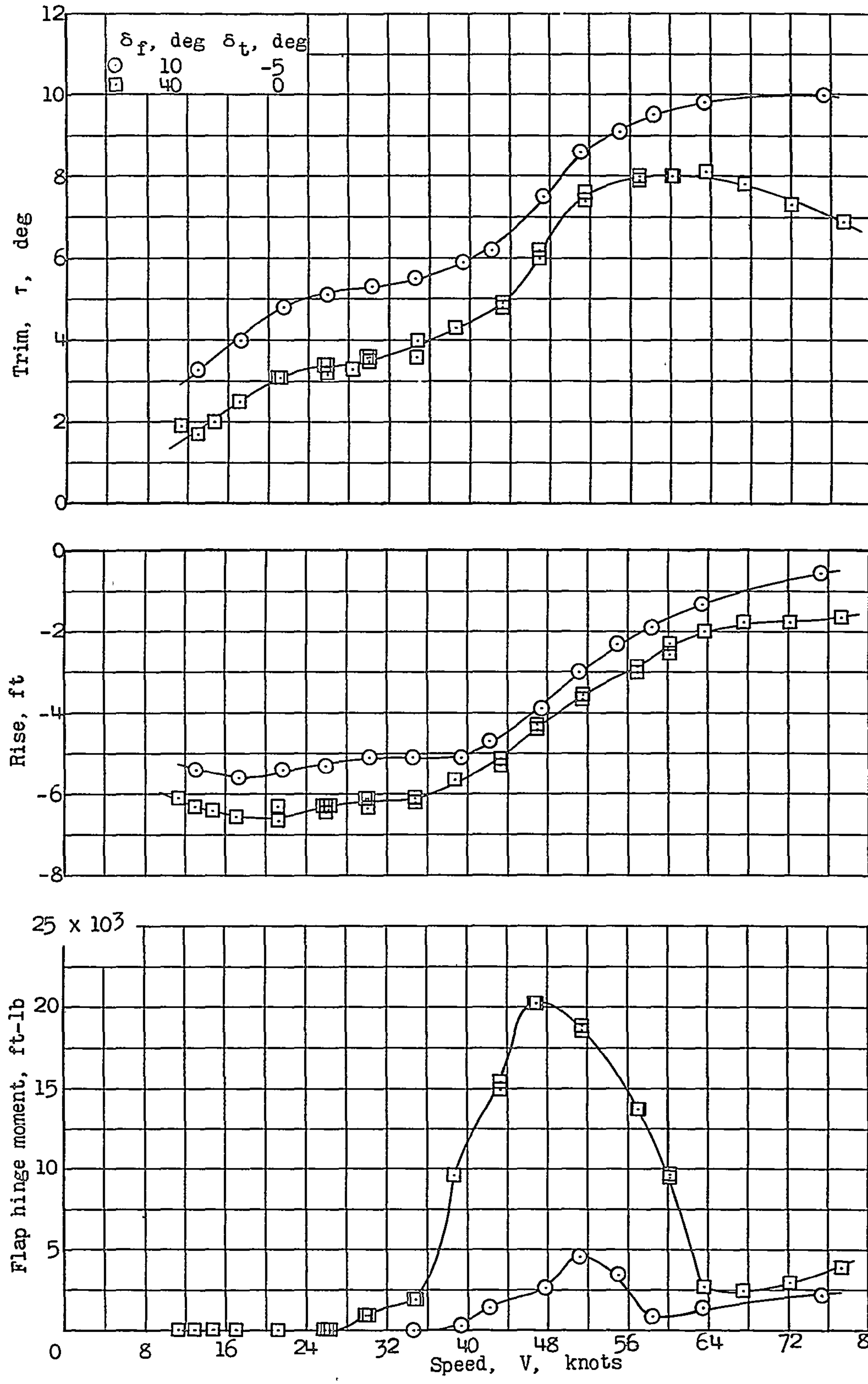

Figure 17.- Variation of trim, rise, and flap hinge moment with speed in smooth water. Δ_o = 160,000 pounds. Langley tank model 316.

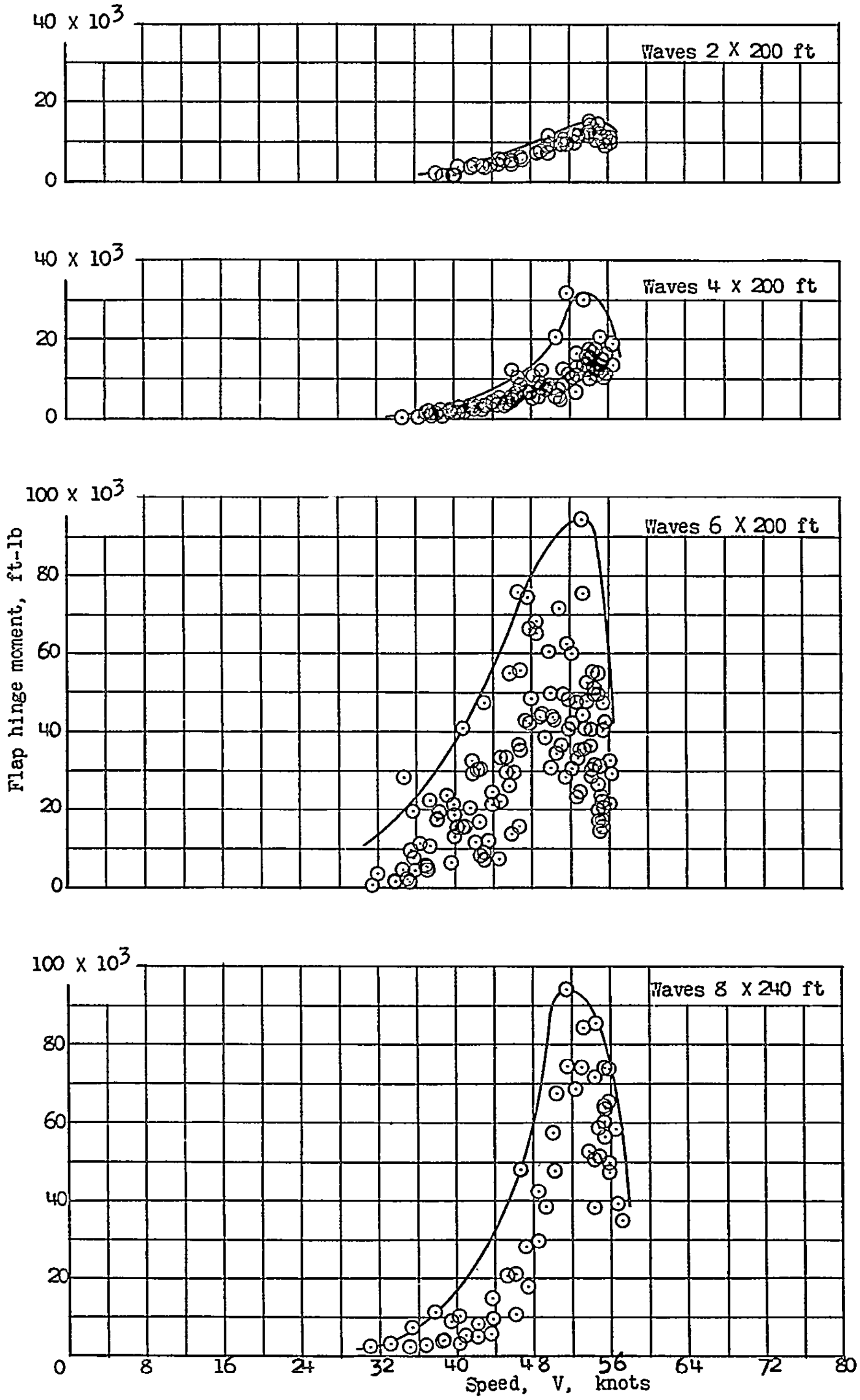

(a) Taxiing; $\delta_f = 10^{\circ}$; power on.

Figure 18.- Variation of flap hinge moment with speed in rough water. $\Delta_o = 160{,}000$ pounds. Langley tank model 316.

[redacted]

[redacted]

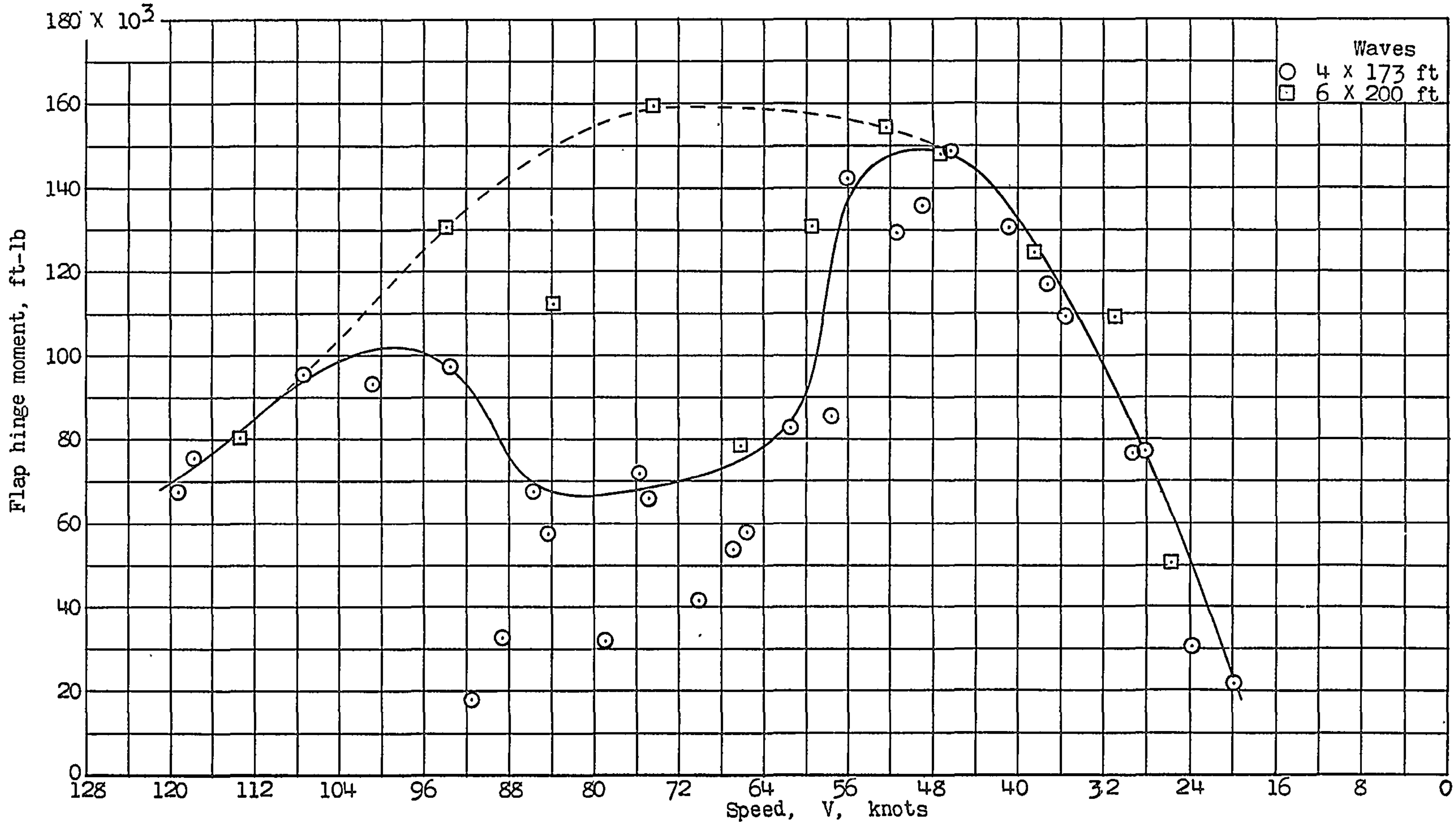

(b) Landing; $\delta_f = 40^{\circ}$; power off.

Figure 18.- Concluded.

[redacted]

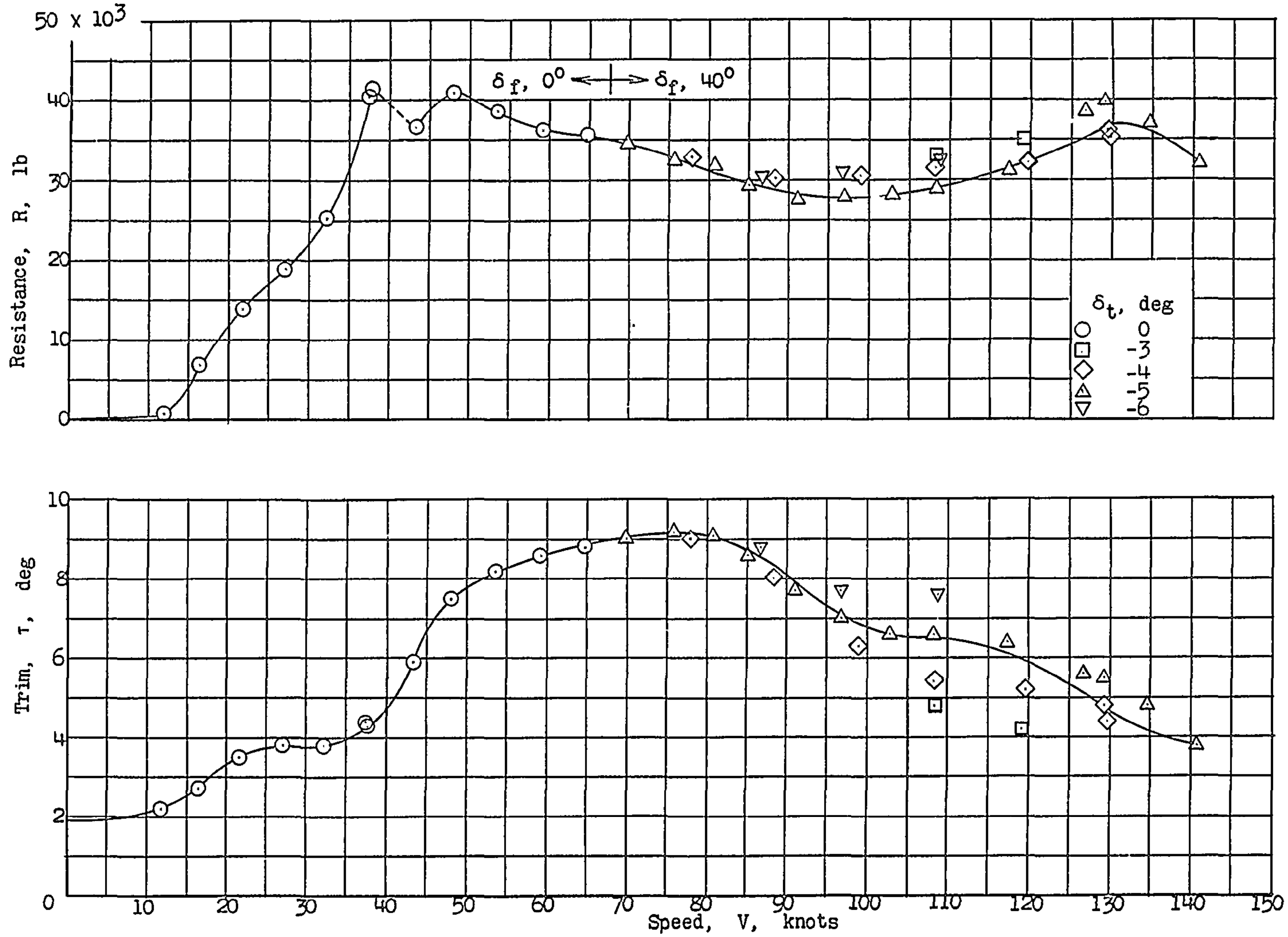

Figure 19.- Minimum total resistance and best trim. Gross load = 160,000 pounds; power off. Langley tank model 316.

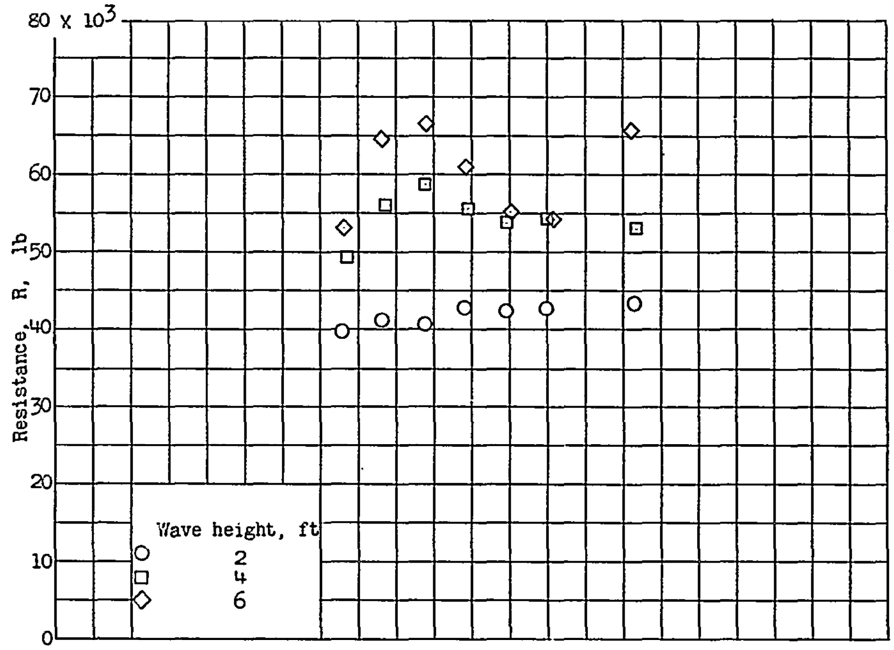

(a) Flap deflection, 0°

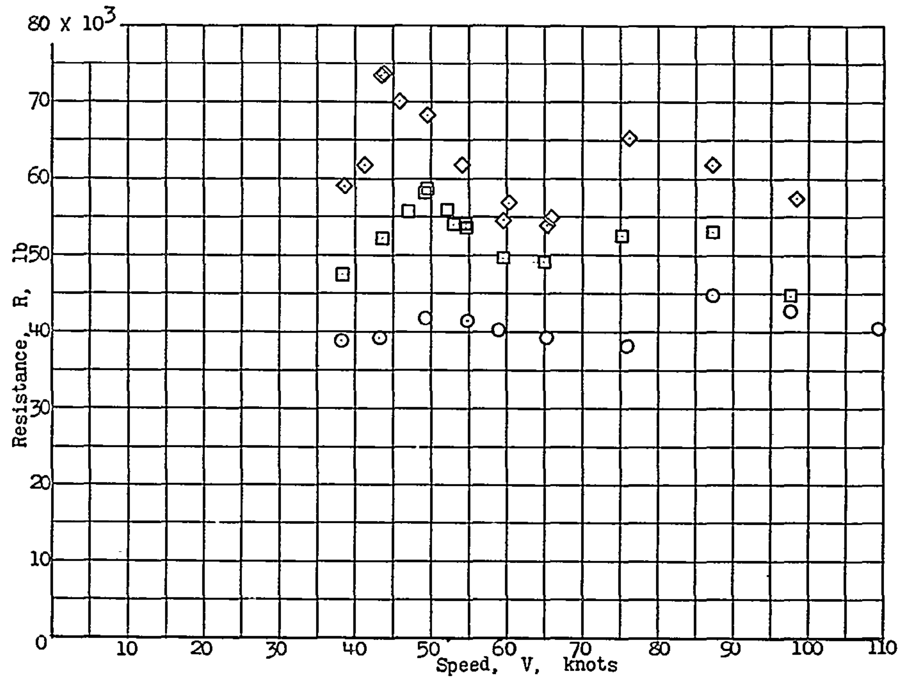

(b) Flap deflection, 10°.

Figure 20.- Effect of wave height on average total resistance in rough water. $\Delta_0 = 160{,}000$ pounds; power off; wave length = 200 feet. Langley tank model 316-5.

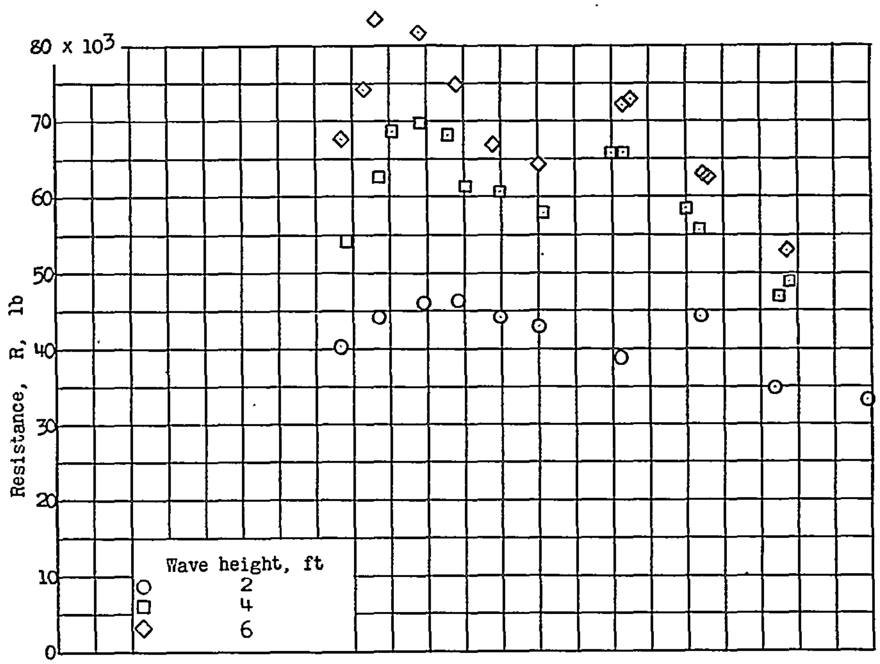

(c) Flap deflection, 40°.

Figure 20.- Concluded.

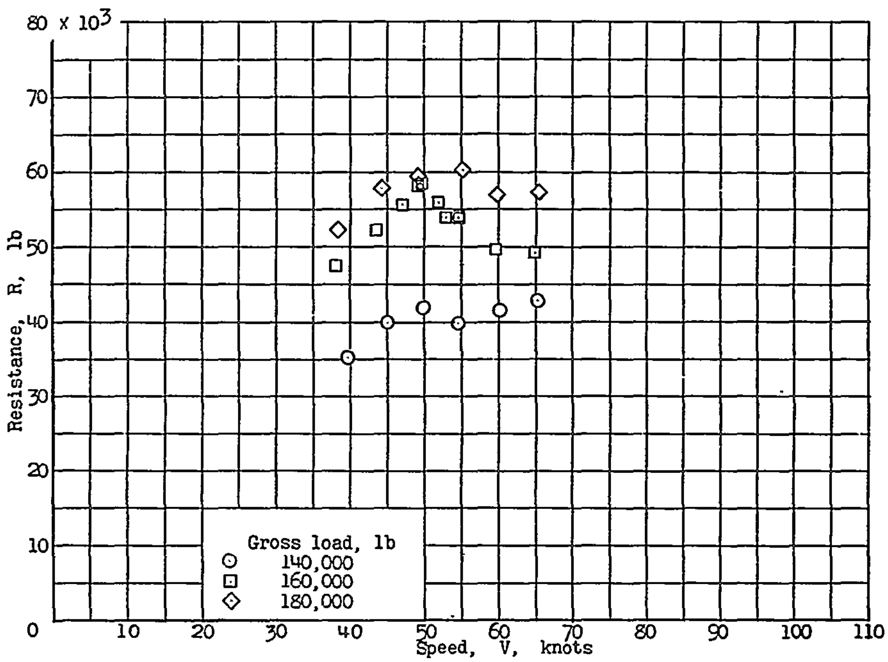

Figure 21.- Effect of gross load on total resistance in rough water. Flap deflection = 10°; power off; wave height = 4 feet; wave length = 200 feet. Langley tank model 316-5.

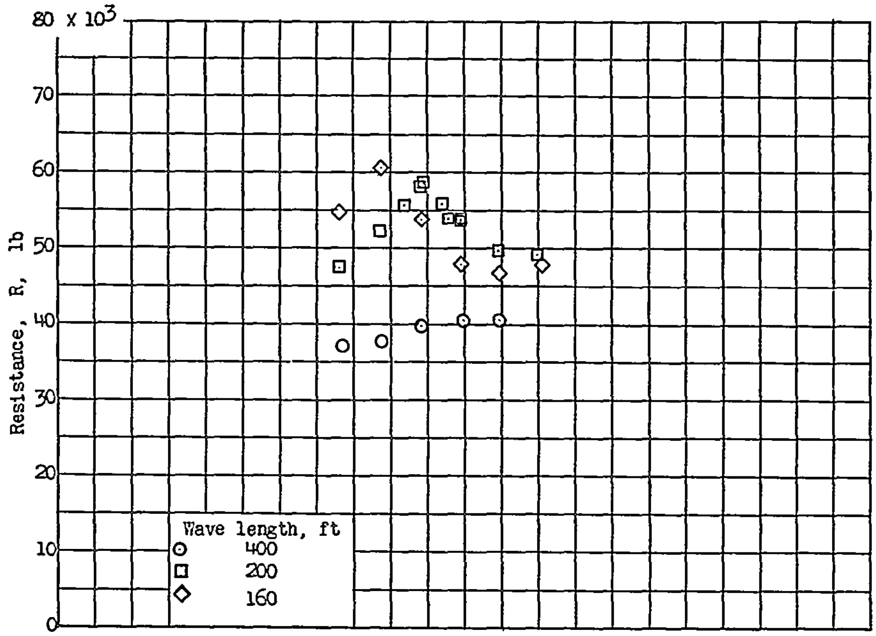

(a) Wave height, 4 feet.

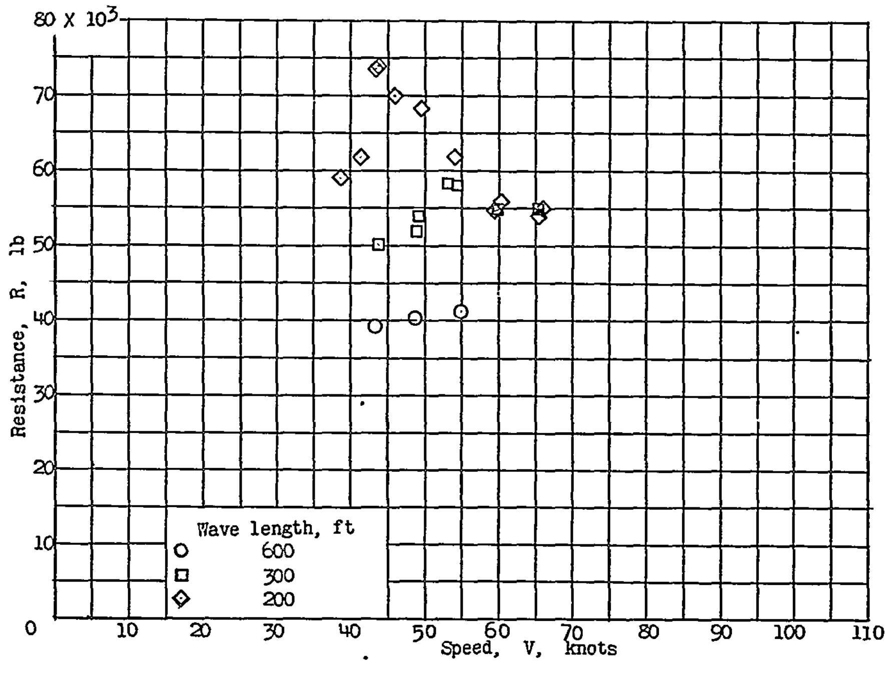

(b) Wave height, 6 feet.

Figure 22.- Effect of wave length on total resistance in rough water. Δ_o = 160,000 pounds; flap deflection = 10°; power off. Langley tank model 316-5.

 [redacted]

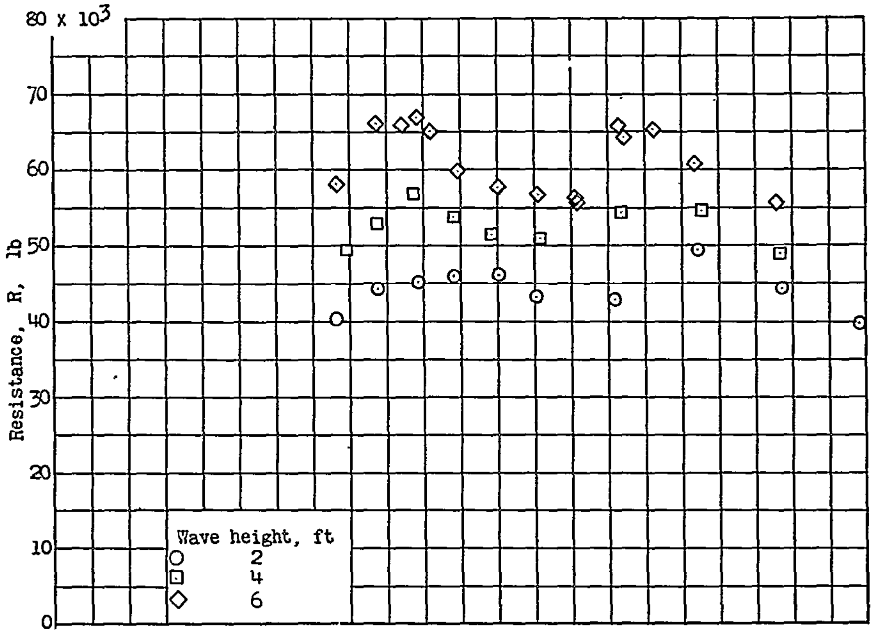

(a) Flap deflection, 10°.

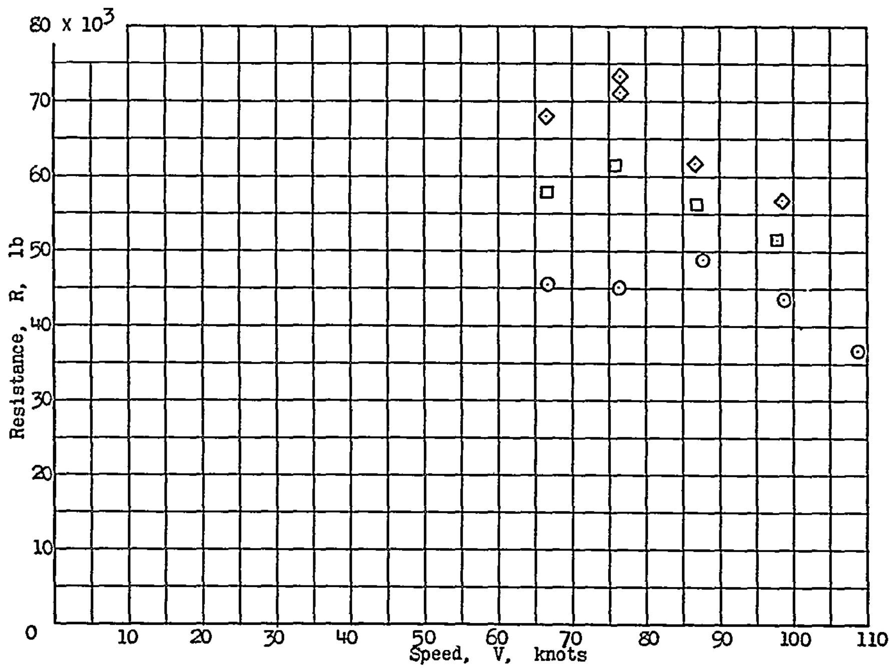

(b) Flap deflection, 40°.

Figure 23.- Effect of wave height on total resistance in rough water. Δ_0 = 160,000 pounds; power off; wave length = 200 feet. Langley tank model 316-12.

[redacted]

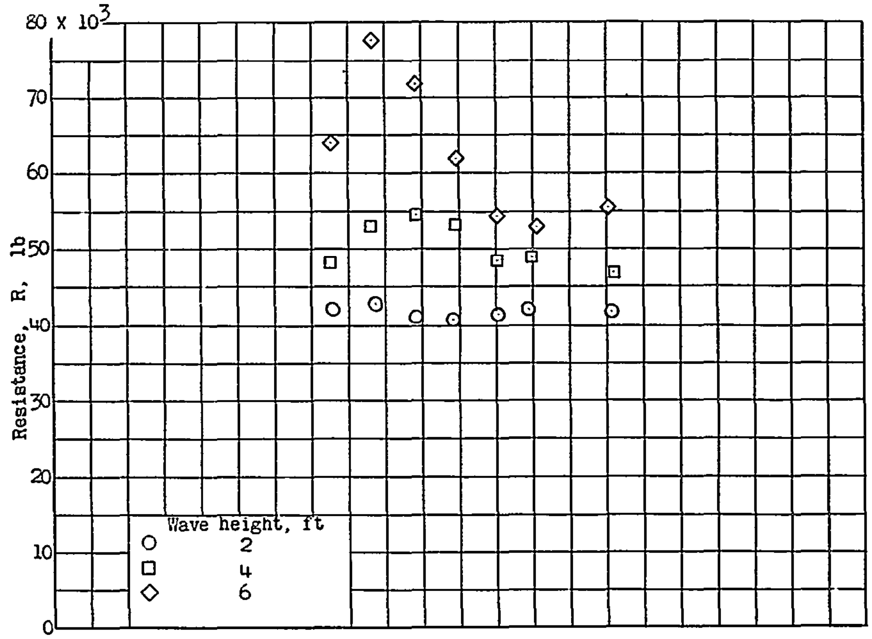

(a) Flap deflection, 10°.

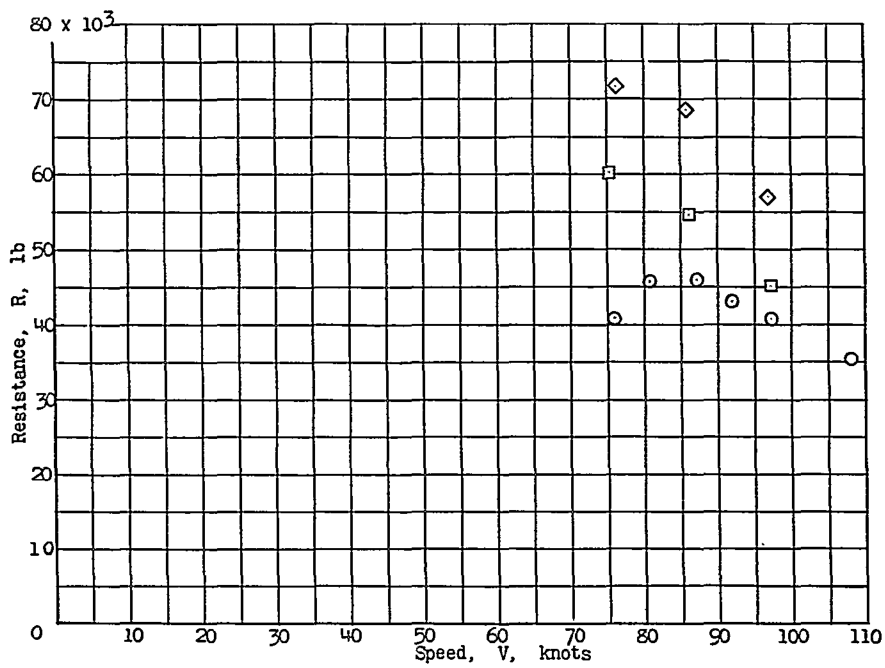

(b) Flap deflection, 40°.

Figure 24.- Effect of wave height on total resistance in rough water. Δ_0 = 160,000 pounds; power off; wave length = 200 feet. Langley tank model 316-13.

[redacted]